



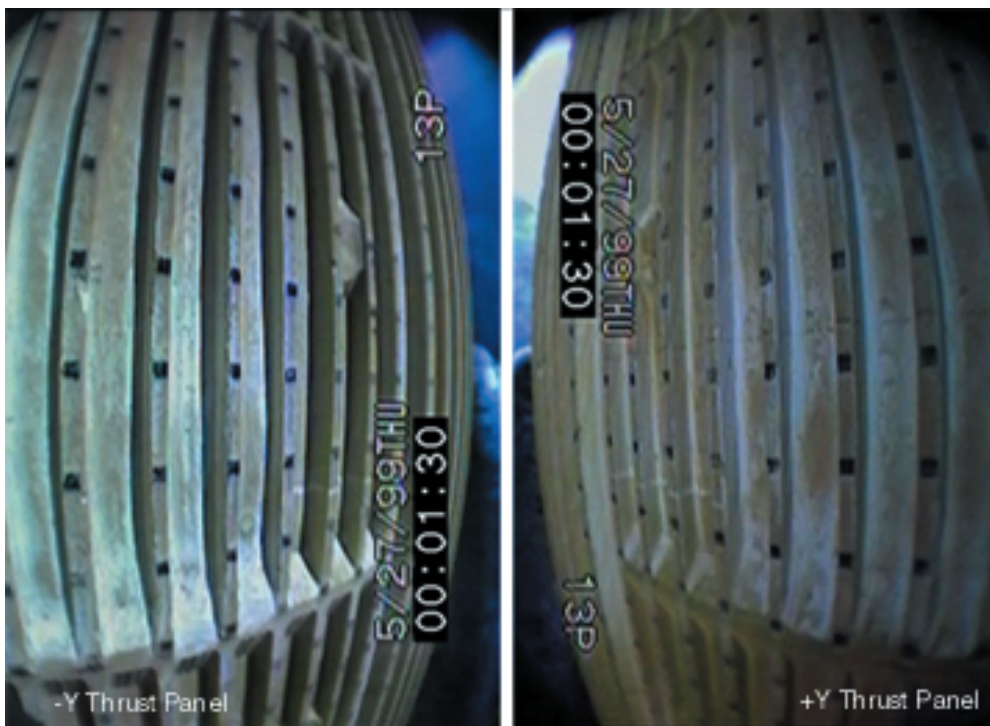
Photographic Analysis Technique for Assessing External Tank Foam Loss Events

T.J. Rieckhoff

Marshall Space Flight Center, Marshall Space Flight Center, Alabama

M. Covan and J.M. O'Farrell

United Space Alliance, Huntsville, Alabama



The NASA STI Program Office...in Profile

Since its founding, NASA has been dedicated to the advancement of aeronautics and space science. The NASA Scientific and Technical Information (STI) Program Office plays a key part in helping NASA maintain this important role.

The NASA STI Program Office is operated by Langley Research Center, the lead center for NASA's scientific and technical information. The NASA STI Program Office provides access to the NASA STI Database, the largest collection of aeronautical and space science STI in the world. The Program Office is also NASA's institutional mechanism for disseminating the results of its research and development activities. These results are published by NASA in the NASA STI Report Series, which includes the following report types:

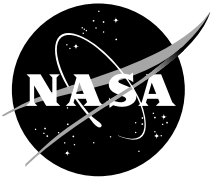
- **TECHNICAL PUBLICATION.** Reports of completed research or a major significant phase of research that present the results of NASA programs and include extensive data or theoretical analysis. Includes compilations of significant scientific and technical data and information deemed to be of continuing reference value. NASA's counterpart of peer-reviewed formal professional papers but has less stringent limitations on manuscript length and extent of graphic presentations.
- **TECHNICAL MEMORANDUM.** Scientific and technical findings that are preliminary or of specialized interest, e.g., quick release reports, working papers, and bibliographies that contain minimal annotation. Does not contain extensive analysis.
- **CONTRACTOR REPORT.** Scientific and technical findings by NASA-sponsored contractors and grantees.

- **CONFERENCE PUBLICATION.** Collected papers from scientific and technical conferences, symposia, seminars, or other meetings sponsored or cosponsored by NASA.
- **SPECIAL PUBLICATION.** Scientific, technical, or historical information from NASA programs, projects, and mission, often concerned with subjects having substantial public interest.
- **TECHNICAL TRANSLATION.** English-language translations of foreign scientific and technical material pertinent to NASA's mission.

Specialized services that complement the STI Program Office's diverse offerings include creating custom thesauri, building customized databases, organizing and publishing research results...even providing videos.

For more information about the NASA STI Program Office, see the following:

- Access the NASA STI Program Home Page at <http://www.sti.nasa.gov>
- E-mail your question via the Internet to help@sti.nasa.gov
- Fax your question to the NASA Access Help Desk at (301) 621-0134
- Telephone the NASA Access Help Desk at (301) 621-0390
- Write to:
NASA Access Help Desk
NASA Center for Aerospace Information
7121 Standard Drive
Hanover, MD 21076-1320
(301)621-0390



Photographic Analysis Technique for Assessing External Tank Foam Loss Events

T.J. Rieckhoff

Marshall Space Flight Center, Marshall Space Flight Center, Alabama

M. Covan and J.M. O'Farrell

United Space Alliance, Huntsville, Alabama

National Aeronautics and
Space Administration

Marshall Space Flight Center • MSFC, Alabama 35812

Acknowledgments

The authors would like to acknowledge Steven Holmes and Jay Sambamurthi for their help in obtaining information about foam loss events and especially their guidance in organizing and formatting results of this investigation. We would also like to thank Lee Foster for enlightening discussions about the nature of foam loss events that aided in formulation of methods used on this project and for help in preparing this Technical Memorandum. We wish to thank Mary Ann Jefferson and Susan Burrer, editors, and Mary Chou, illustrator, Marshall Space Flight Center, Scientific and Technical Publications, for their insightful comments and expert help in preparation of this document.

Available from:

NASA Center for AeroSpace Information
7121 Standard Drive
Hanover, MD 21076-1320
(301) 621-0390

National Technical Information Service
5285 Port Royal Road
Springfield, VA 22161
(703) 487-4650

TABLE OF CONTENTS

1. INTRODUCTION	1
2. SOLID ROCKET BOOSTER CAMERA	4
3. EVALUATION METHOD OVERVIEW	6
4. DIFFERENCING TECHNIQUE	7
5. CATEGORIZATION OF FOAM LOSS EVENTS	10
6. RESULTS	11
6.1 STS-95 -Y Thrust Panel	12
6.2 STS-96/ET-100 -Y Thrust Panel	14
6.3 STS-96/ET-100 +Y Thrust Panel	17
6.4 STS-93/ET-99 -Y Thrust Panel	20
6.5 STS-93/ET-99 +Y Thrust Panel	23
6.6 STS-103 -Y Thrust Panel	26
6.7 STS-103 +Y Thrust Panel	29
6.8 STS-101 -Y Thrust Panel	32
6.9 STS-101 +Y Thrust Panel	35
7. DISCUSSION	38
BIBLIOGRAPHY	41

LIST OF FIGURES

1.	SOFI over intertank ribs	1
2.	STS–87/ET–89 foam loss from intertank	2
3.	Machined and vented foam	3
4.	SRB camera	4
5.	View of ET thrust panel from SRB camera	5
6.	Schematic of directed differences	9
7.	Difference image example	9
8.	Masks applied to thrust panel images	10
9.	STS–95 –Y thrust panel	12
10.	STS–95 –Y thrust panel: Foam loss event timeline	13
11.	STS–95 –Y thrust panel: Foam loss timeline for categories of events	13
12.	STS–96 –Y thrust panel	14
13.	STS–96 –Y thrust panel: Foam loss event timeline	15
14.	STS–96 –Y thrust panel: Foam loss timeline for vented and nonvented areas	15
15.	STS–96 –Y thrust panel: Foam loss timeline for categories of events	16
16.	STS–96 +Y thrust panel	17
17.	STS–96 +Y thrust panel: Foam loss event timeline	18
18.	STS–96 +Y thrust panel: Foam loss timeline for vented and nonvented areas	18
19.	STS–96 +Y thrust panel: Foam loss timeline for categories of events	19
20.	STS–93 –Y thrust panel	20

LIST OF FIGURES (Continued)

21.	STS-93 -Y thrust panel: Foam loss event timeline	21
22.	STS-93 -Y thrust panel: Foam loss timeline for vented and nonvented areas	21
23.	STS-93 -Y thrust panel: Foam loss event timeline for categories of events	22
24.	STS-93 +Y thrust panel	23
25.	STS-93 +Y thrust panel: Foam loss event timeline	24
26.	STS-93 +Y thrust panel: Foam loss timeline for vented and nonvented areas	24
27.	STS-93 +Y thrust panel: Foam loss timeline for categories of events	25
28.	STS-103 -Y thrust panel	26
29.	STS-103 -Y thrust panel: Foam loss event timeline	27
30.	STS-103 -Y thrust panel: Foam loss timeline for vented and nonvented areas	27
31.	STS-103 -Y thrust panel: Foam loss timeline for categories of events	28
32.	STS-103 +Y thrust panel	29
33.	STS-103 +Y thrust panel: Foam loss event timeline	30
34.	STS-103 +Y thrust panel: Foam loss timeline for vented and nonvented areas	30
35.	STS-103 +Y thrust panel: Foam loss timeline for categories of events	31
36.	STS-101 -Y thrust panel	32
37.	STS-101 -Y thrust panel: Foam loss event timeline	33
38.	STS-101 -Y thrust panel: Foam loss timeline for vented and nonvented areas	33
39.	STS-101 -Y thrust panel: Foam loss timeline for categories of events	34
40.	STS-101 +Y thrust panel	35
41.	STS-101 +Y thrust panel: Foam loss event timeline	36

LIST OF FIGURES (Continued)

42.	STS-101 +Y thrust panel: Foam loss timeline for vented and nonvented areas	36
43.	STS-101 +Y thrust panel: Foam loss timeline for categories of events	37
44.	Foam loss comparison for -Y thrust panels	39
45.	Foam loss comparison for +Y thrust panels	39

LIST OF TABLES

1.	Counting methods differences	38
----	------------------------------------	----

LIST OF ACRONYMS

CCIR	International Radio Consultative Committee
ET	external tank
IFA	in-flight anomaly
MSFC	Marshall Space Flight Center
RGB	red, green, blue (color system)
SOFI	spray-on foam insulation
SRB	solid rocket booster
STA	station (axial position on external tank)
STS	Space Transportation System
TPS	thermal protection system

NOMENCLATURE

b	blue component
g	green component
r	red component
$f(x,y)$	two-dimensional light intensity function
I, J	given image
I_1, I_2	subsequent images
I_p	preceding image
I_s	subsequent image
p, q	pixel
s, t	spatial coordinate
x, y	spatial coordinate
+Y	right-hand side
-Y	left-hand side
δ	difference operator
$\bar{\delta}(q,p)$	directed pixel difference
Δ	image difference operator
$\bar{\Delta}(I,J)$	directed image difference

TECHNICAL MEMORANDUM

PHOTOGRAPHIC ANALYSIS TECHNIQUE FOR ASSESSING EXTERNAL TANK FOAM LOSS EVENTS

1. INTRODUCTION

The external tank (ET) of the Space Shuttle system is covered with a very low-density, spray-on foam insulation (SOFI) to protect it from the heating experienced during ascent flight. The intertank thrust panels (fig. 1) are ribbed structures that resemble corrugated panels when sprayed with foam.

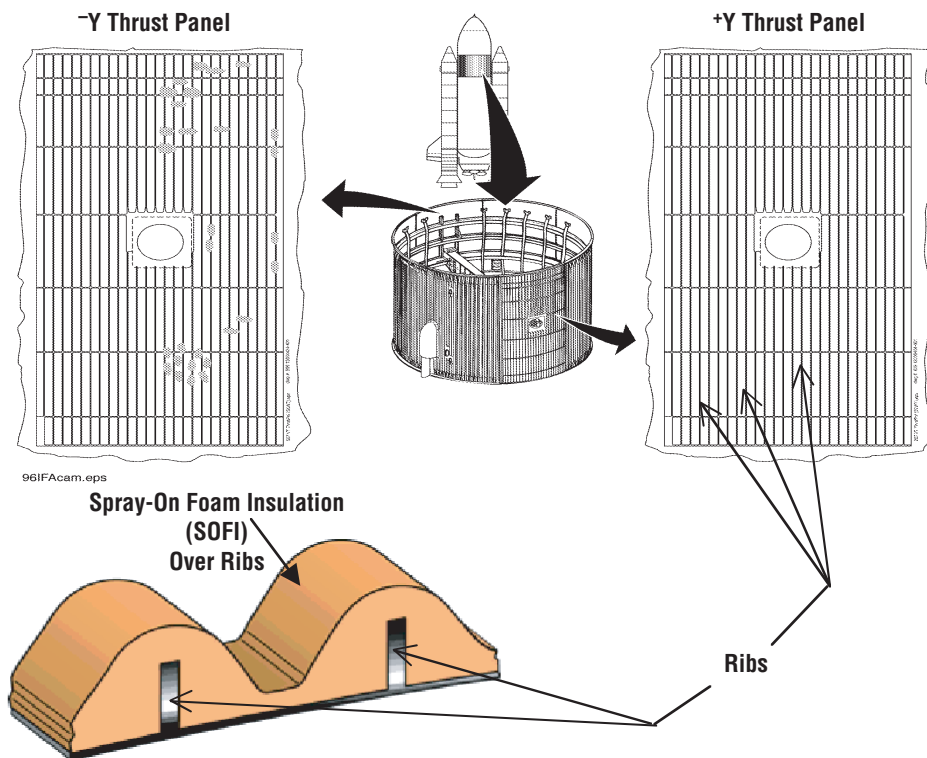


Figure 1. SOFI over intertank ribs.

STS-86/ET-88, launched on September 25, 1997, flew the first ET intertank for which NCFI 24-124 SOFI was used in place of the previous CPR-488. This changeover was due to environmental constraints on the foam-blowing agent used in CPR-488. There are three distinct differences between the foams: (1) A change of the basic polymer from CPR-488 to NCFI 24-124, (2) a change of blowing agent from CFC-11 to the more environmentally friendly HCFC-141b, and (3) a reduction in nominal density of NCFI 24-124 foam to achieve weight reduction goals of the Super Lightweight Tank program.

Postflight inspection of orbiter tiles on mission STS-86 revealed greater damage than observed on previous flights. STS-87/ET-89, launched on November 19, 1997, had even more tile damage and prompted the initiation of in-flight anomaly STS-87-T-01 (IFA87) to identify the cause of the orbiter's above average, lower surface tile damage and suggest corrective action. Foam loss was suspected to be the cause of damage to the orbiter tiles. Figure 2 shows a photograph of the STS-87 ET after it was jettisoned. Areas of foam loss from the intertank are readily apparent.

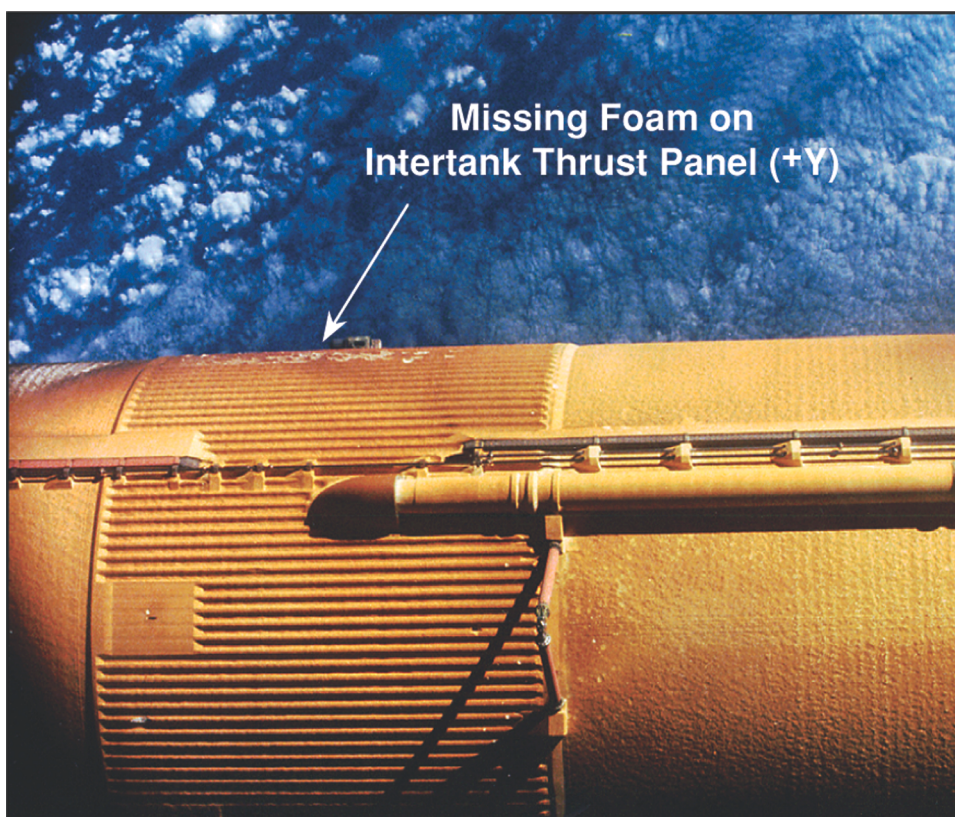


Figure 2. STS-87/ET-89 foam loss from intertank.

The hypothesized main causes of foam loss were (1) reduction in mechanical properties of the foam at elevated temperatures, (2) environmentally induced stresses in the foam (exposure to vacuum and heat during flight combined with exposure to humidity before launch), and (3) stress concentrating geometry of the ET intertank ribs.

For the next several flights, in order to reduce the mechanical stresses on the intertank foam, the foam was sanded or machined down. Several areas were vented to reduce stress due to vacuum and heat (fig. 3).

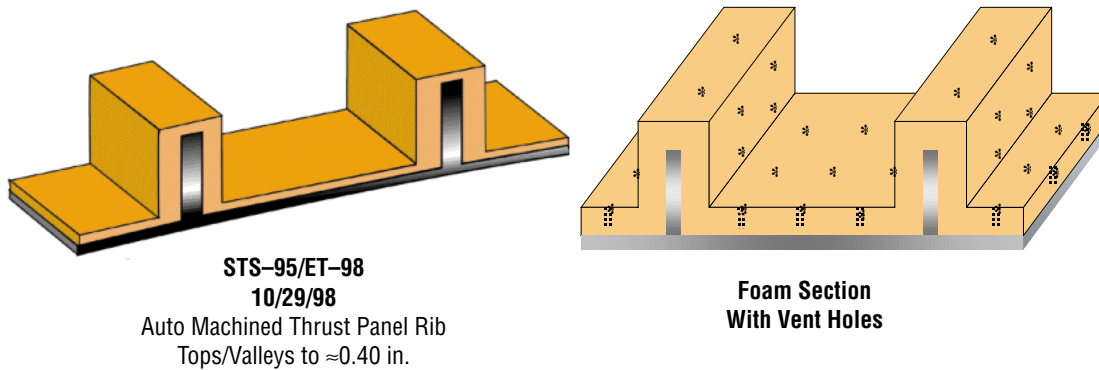


Figure 3. Machined and vented foam.

A camera was installed on the left solid rocket booster (SRB) of STS-95/ET-98, launched on October 29, 1998, providing video images of the ET intertank thrust panels during ascent. From the video, foam loss was seen to initiate at \approx 92 sec into flight and continue until SRB separation, at which time the view was lost. From simple observation of the STS-95 SRB camera video, foam loss appeared to be most prominent on the tops and sides of the thrust panel ribs. It was also noted that from a visual standpoint, the foam loss closely resembled the phenomenon known as popcorning, which has been observed in thermal vacuum testing at Marshall Space Flight Center (MSFC) test facilities.

Tile damage impact testing was conducted by Southwestern Research Laboratories to assess the susceptibility of the orbiter tiles to damage from the ET foam particles. Test results demonstrated that the particles of the size detected in the STS-95 video could cause the observed orbiter tile damage. Flight instrumentation and video cameras were installed on both left and right SRB's for missions STS-96/ET-99 and STS-93/ET-100. Data from the videos were used to identify the times that foam loss occurred and to record differences in foam loss characteristics. The times could then be correlated to environmental conditions experienced by the foam and related to known reasons for foam loss. Also, other reasons for foam loss might be illuminated.

Several initial efforts were made to determine foam loss events by simply viewing the video and marking changes that corresponded to foam loss events. The position of the foam loss events was determined using a system of grid marks placed on the ET intertank thrust panels. These assessments resulted in varying counts of foam loss events. MSFC engineering photographic analysis personnel were asked to aid in quantifying the number, size, location, and time of the foam loss events recorded by the SRB videos.

A method of processing the SRB video images was developed to allow rapid detection of permanent changes indicative of foam loss events on the ET intertank surface. This method was applied to accurately time, count, categorize, and locate changes corresponding to foam loss events.

2. SOLID ROCKET BOOSTER CAMERA

A standard 8-mm video camera with a separate recorder located inside the SRB forward skirt was used to obtain images of the ET thrust panel during flight. The image views an area on the ET intertank roughly between locations STA 952 and STA 1035 (fig. 4). The camera is a Super Circuit model PC-17YC with a 4.3-mm focal length with f1.8 lens aperture, a 74-deg field of view, and 450 horizontal lines of resolution. The camera iris is automatically controlled and the focus is manually set and locked for each flight. The recorder is a Sony model EV0220. The camera and recorder are activated in flight by a 2G switch. The recording time lasts from approximately L+5 sec until SRB splashdown.

As an aid in visual determination of the location and size of foam loss events, grid marks were applied to the intertank from the intertank ET/SRB fitting to the rib/stringer panel splice. The field of view and grid marker symbols, *, used on flight STS-95, are shown in figure 5. Each grid mark symbol, is 1 in. in diameter. On flights subsequent to STS-95, grid mark symbols were made with 1-in.-square blocks. These grid marks may be observed in the images of the ET intertank thrust panel on those flights.

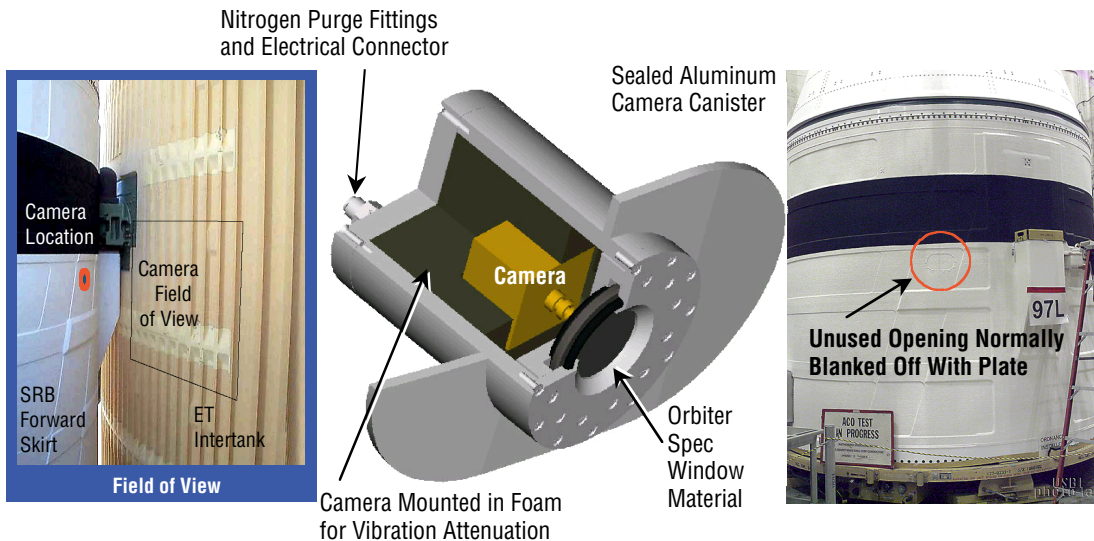


Figure 4. SRB camera.



Figure 5. View of ET thrust panel from SRB camera.

3. EVALUATION METHOD OVERVIEW

The process for generating information about permanent thermal protection system (TPS) loss events was accomplished in several stages. A source Betacam SP-formatted videotape, copied from the original SRB camera's videotape, was obtained and digitized in CCIR 601 component standard image format.

Rather than evaluate each frame or field of video data over the time period between T+5 sec and splashdown, frames were selected at 0.5-sec intervals from T+90 sec until SRB separation. This time period encompassed nearly all changes to the ET surface that resulted in foam loss events on the ET thrust panels. Before T+90 sec, no noticeable changes were evident on the ET surface. After SRB separation, the cameras rapidly moved away from the ET and the wide field of view rendered the image too small to accurately evaluate ET surface changes.

The even field was extracted from each digitized video image and interpolated to produce an image of the same size as the original image. The differencing technique, developed to aid in the detection of ET foam loss events, was applied to these deinterlaced images. This resulted in a sequence of images in which permanent ET surface changes were highlighted.

Each image was reviewed and areas judged to correspond to ET TPS foam loss events were highlighted and their location recorded. The differencing technique is discussed in section 4 and results for each flight are detailed in the associated section.

4. DIFFERENCING TECHNIQUE

An image is a two-dimensional light intensity function, $f(x,y)$, where x and y denote spatial coordinates. The value of the function $f(x,y)$ is a three-dimensional vector, with each component proportional to color intensity at that spatial coordinate. The color intensity of each component is a positive number between 0 and 255. Using the red, green, blue (RGB) color system, the first vector coordinate corresponds to the intensity of the color red, the second to the intensity of the color green, and the third to the intensity of the color blue. A digital image is a discretized light intensity function. Standard video images are digitized into a 720×486 array where each element of the array is called a pixel. The value of a pixel is the value of the discretized light intensity function at the pixel x,y array coordinates.

Given two pixels, p at location (x,y) and q at location (s,t) , their difference, $\delta(q,p)$, is the absolute value of the difference of each component of their light intensity functions:

$$\begin{aligned}\delta(q,p) &= |f_p(x,y) - f_q(s,t)| \\ &= (|r_p - r_q|, |g_p - g_q|, |b_p - b_q|) \quad .\end{aligned}\quad (1)$$

Given two images I and J , the difference between I and J is denoted $\Delta(I,J)$:

$$\Delta(I,J) = \left\{ \delta(p_I, p_J) : \begin{array}{l} \text{Spatial location of } p_I = \text{spatial location of } p_J \\ p_I \text{ is in image } I \text{ and } p_J \text{ is in image } J \end{array} \right\} \quad .\quad (2)$$

This straightforward difference image $\Delta(I,J)$ records all changes between two images. Changes in light intensity, debris motion, and motion of the frame resulting from vibration are typical events which are revealed in the straightforward difference image.

In this study, a directed pixel difference, $\bar{\delta}(q,p)$, and corresponding directed image difference, $\bar{\Delta}(I,J)$, was used, where

$$\bar{\delta}(p,q) = \min \left\{ \max(r_q - r_p, 0) \max(g_q - g_p, 0) \max(b_q - b_p, 0) \right\} \quad (3)$$

and

$$\bar{\Delta}(I,J) = \left\{ \bar{\delta}(p_I, p_J) : \begin{array}{l} \text{Spatial location of } p_I = \text{spatial location of } p_J \\ p_I \text{ is in image } I \text{ and } p_J \text{ is in image } J \end{array} \right\} \quad .\quad (4)$$

To reference the directed difference, using a pixel (x,y) spatial location between two images I and J of the same size, the following notation is used:

$$\bar{\Delta}(I,J)[x,y] \quad . \quad (5)$$

The directed pixel difference is equivalent to the least nonnegative value for the maximum of zero and each of the component values of the vector subtraction of the q pixel from the p pixel. The difference provides a time-directed, single-comparison value for each pixel, which is ≥ 0 . When the surface material of the ET is removed, the exposed foam is a lighter color than the surface foam. Light ET surface areas that turn dark in successive images appeared not to be associated with a foam loss event. The directed difference discriminated against these types of changes in surface intensity.

By employing a suitable threshold value for the function $\bar{\Delta}(I,J)$, most of the inherent video noise may be screened, yet significant ET surface changes registered. A gray level of 20 was chosen as the threshold value for $\bar{\Delta}(I,J)$ in these investigations; i.e., for a specific pixel in an image, the directed difference in intensity levels for that pixel in each color band between the two images was required to be >20 .

In order to differentiate permanent events from transient events, four images were used in the differencing technique: A given image, I ; its preceding image, I_p ; and its two subsequent images, I_{s1} and I_{s2} . A change for a given pixel spatial location (x,y) was designated as permanent given that the following conditions were met:

- (1) $\bar{\Delta}(I_p, I)[x,y] > 0$, which ensured that a change had occurred between image I and I_p at the pixel with spatial location (x,y)
- (2) $\bar{\Delta}(I, I_{s1})[x,y] = 0$, which implies that the change was relatively persistent
- (3) $\bar{\Delta}(I_p, I_{s1})[x,y] > 0$, $\bar{\Delta}(I_p, I_{s2})[x,y] > 0$, $\bar{\Delta}(I, I_{s2})[x,y] = 0$, and $\bar{\Delta}(I_{s1}, I_{s2})[x,y] = 0$ redundancy tests to ensure persistence of the detected change.

The first condition is necessary for a change between two images. The second condition is necessary for detecting changes that are normally persistent in the ET surface. The third conditions are redundancy checks. Occasionally an event that registered as permanent under the second condition turned out to not be a permanent event. Moving objects, videotape motion, and lighting changes fall into this category. The third set of conditions extends the persistency test. When foam popped from the ET surface, the rapidly moving foam usually appeared as a light-colored area in the difference files. Using the redundancy tests, the time interval over which the test conditions were applied was extended to 1 sec and object motion was eliminated as a permanent event. Figure 6 shows the directed differences schematic.

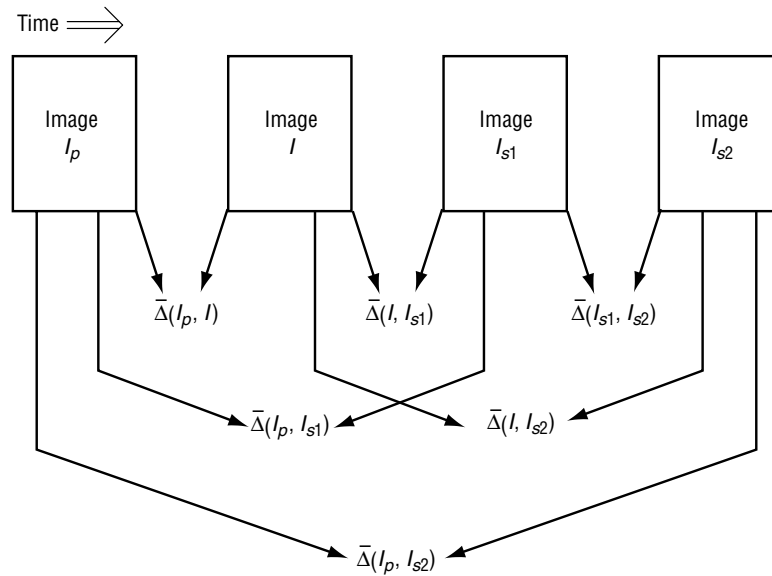


Figure 6. Schematic of directed differences.

The basic directed difference images, illustrated in figure 7, clearly show changes in the ET surface. The full directed difference method screened many events that were not associated with permanent changes in the ET surface and detected most foam loss events. This allowed actual foam loss events to be manually located and their position recorded. Bold coloring of probable foam loss events in the original image was used as a recursive aid in subsequent event addition and verification reviews. This process resulted in a high confidence in the number and location of observed TPS foam loss events. In figure 7, RGB pixel value differences between frames A and B appear in frame C, the difference frame. The greater the difference, the lighter the color. Changes between frames A and B that indicate ET foam loss events are pointed out by arrows in frame B.

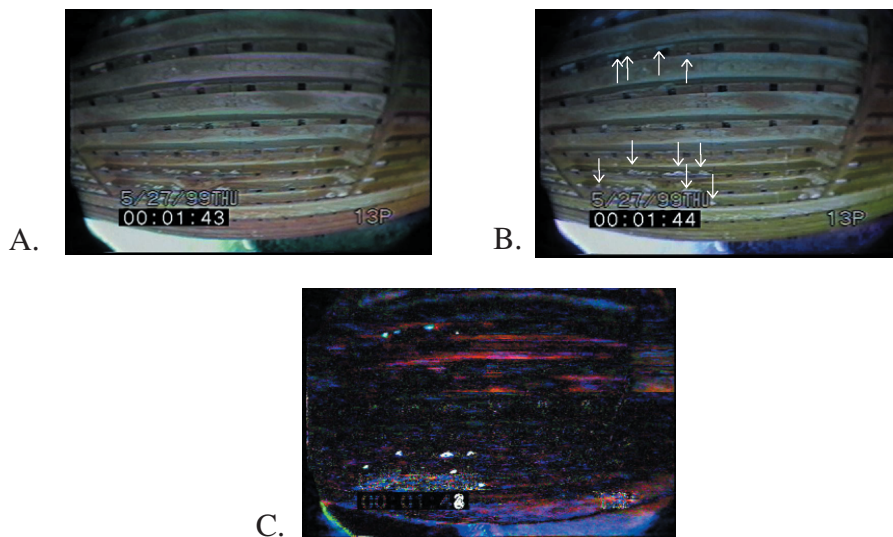


Figure 7. Difference image example.

5. CATEGORIZATION OF FOAM LOSS EVENTS

Several categories of ET surfaces were evaluated for foam loss events, and masks for each of the categories were created. These categories included the process type categories such as vented versus nonvented areas, and positional type categories such as stringers, valleys between ribs, longitudinal ribs, circumferential ribs, and ramps leading to the circumferential ribs. The masks employed color coding to differentiate the specific areas of an image. If the position of a foam loss event is located within the boundaries of a specific color of a mask, the event is marked as belonging to the associated category. Final images for evaluation included the masks blended into the video sequence to highlight categories and facilitate visual identification of foam loss categories.

Example masks applied to an original image in order to extract information about location of the event are illustrated in figure 8. Two separate masks were constructed for each camera on each flight. Mask A is a color coding of the several types of surfaces found on the ET and an event boundary mask (black area) marking the area of the image where changes may be considered as foam loss events. Areas such as the date, time, and nonexternal tank regions were masked from consideration. Illustrated in this example are valleys between the longitudinal ribs, longitudinal ribs, circumferential ribs, the hi-lock region, and ramps leading to the circumferential ribs. Mask B differentiates the area of the ET surface that has been vented from the nonvented surface. The vented area in mask B is black.

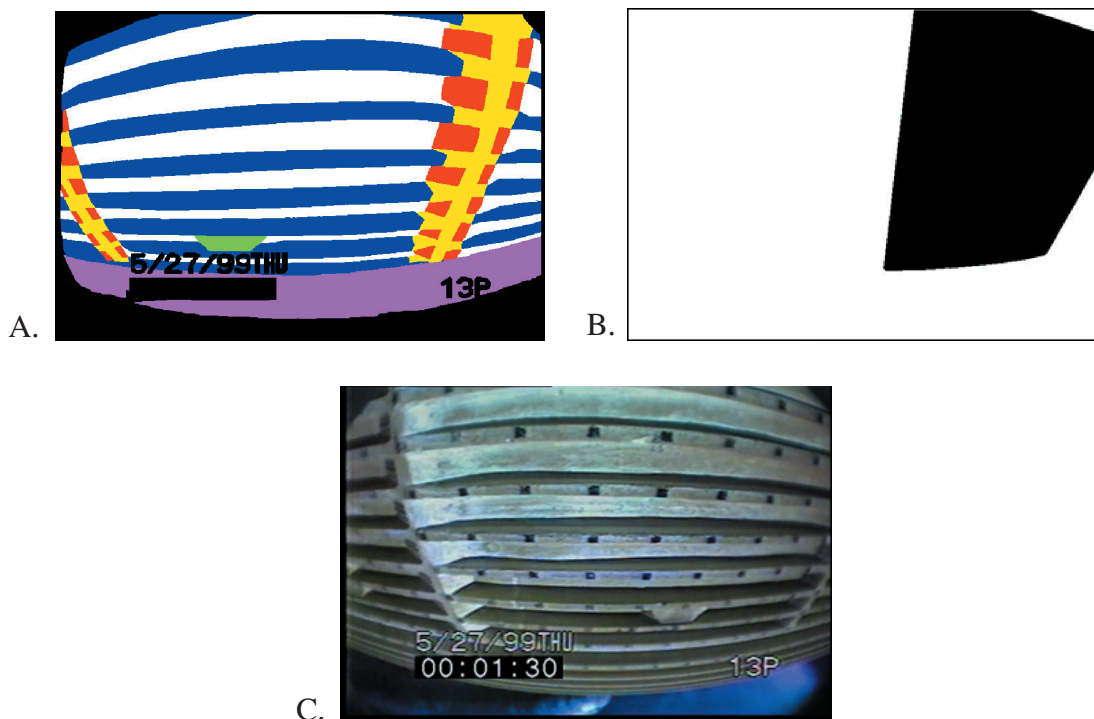


Figure 8. Masks applied to thrust panel images.

6. RESULTS

There have been five Space Shuttle flights on which SRB cameras have flown:

- (1) STS–95 was launched on October 29, 1998, 2:19:34 p.m. e.d.t. STS–95 carried one SRB camera with its field of view on the -Y thrust panel.
- (2) STS–96 was launched on May 27, 1999, 6:49:42 a.m. e.d.t. STS–96 carried two SRB cameras, one viewing each thrust panel. STS–96 flight-tested venting of the foam as a solution to foam loss events.
- (3) STS–93 was launched on July 23, 1999, at 12:31:00 a.m. e.d.t. STS–93 carried two SRB cameras. STS–93 was an *International Space Station* mission and most such flights will be launched at night. It was determined prior to flight that the light intensity from the SRB plumes for a night launch would be sufficient for illumination of the ET surface. However, the average light intensity for this night flight was not as constant as during a day launch. To account for this significant average intensity variation, the difference algorithm threshold was adjusted for several images, dropping the threshold in dark images and increasing the threshold for lighter images.
- (4) STS–103 was launched on December 19, 1999, at 7:49:59 p.m. e.s.t. STS–103 carried two SRB cameras. Extensive venting of the foam was performed on this mission.
- (5) STS–101 was launched on May 19, 2000, at 6:11 a.m. e.d.t. STS–101 carried two SRB cameras. The same venting of the foam was performed on this mission as on mission STS–103.

The following results are included for each flight: (1) A final image of the ET thrust panel with the recorded foam loss events colored bright red, and (2) timelines for all events (vented and nonvented) and event categories.

Due to the rugged environment, camera motion was inevitable. Besides the normal frame-to-frame motion of the video, it was noticed that the camera field of view moved a small, but noticeable, amount during the time period during flight of the study. This may be seen as light areas to the right side of several of the red-colored foam loss events.

6.1 STS-95 -Y Thrust Panel

Figure 9 illustrates all foam loss events tabulated on flight STS-95. The number of events recorded during each 0.5-sec time interval and the total number of events from T+90 sec are shown in figure 10. There were 226 total foam loss events recorded. A fifth-order polynomial trend line for the number of events counted per each 0.5 sec indicates a peak value just after 110 sec. The maximum number of foam loss events in any 0.5-sec time interval was 11.

The ET thrust panel on flight STS-95 was not vented. Figure 11 illustrates the accumulated foam loss in each category of events versus time. There were no recorded events in the ramp area or the circumferential rib area.

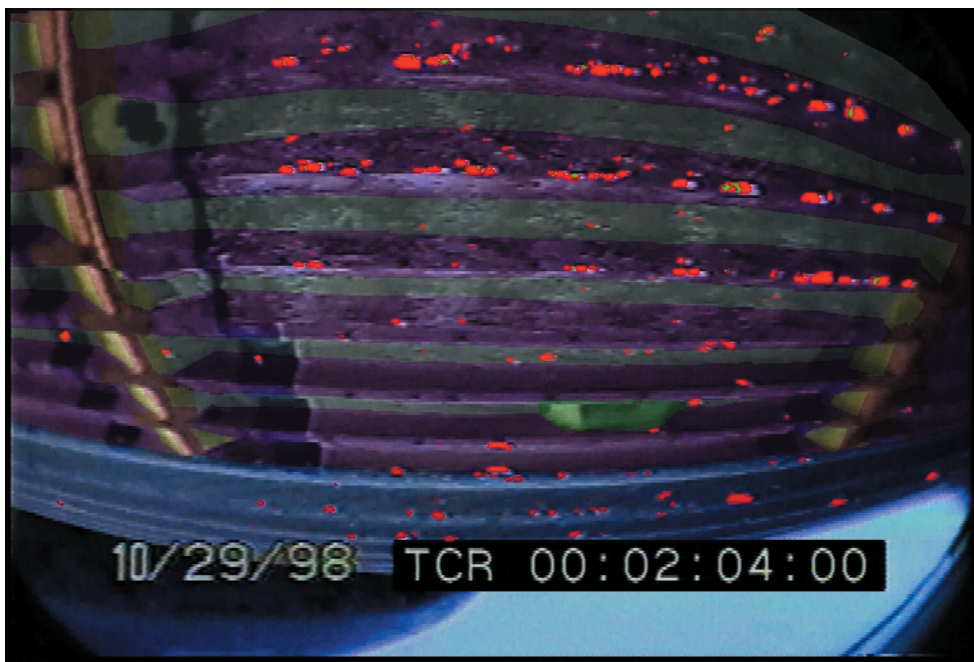


Figure 9. STS-95 -Y thrust panel.

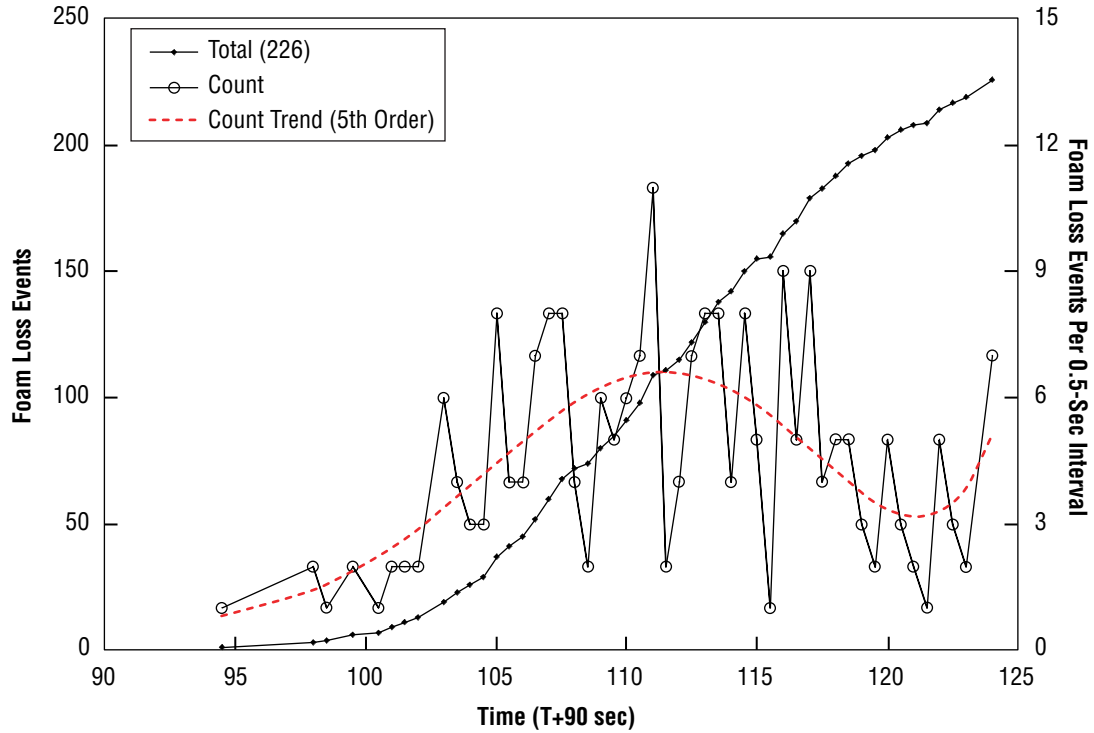


Figure 10. STS-95 -Y thrust panel: Foam loss event timeline.

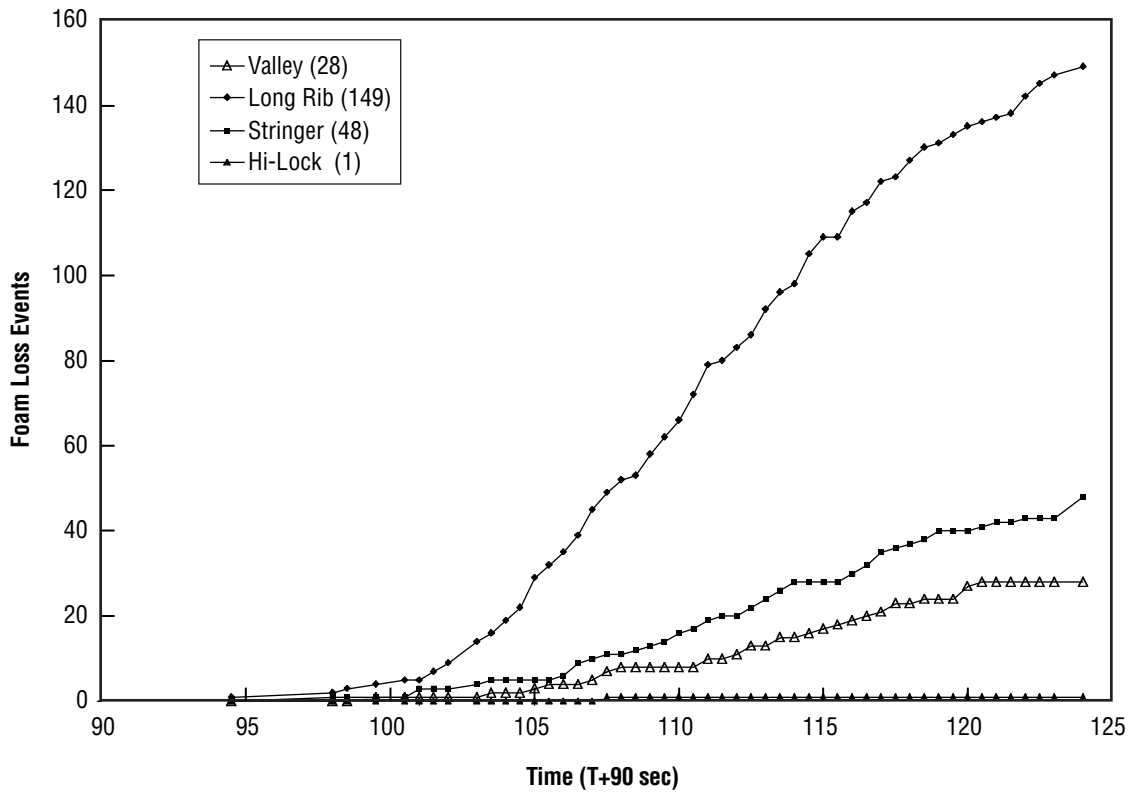


Figure 11. STS-95 -Y thrust panel: Foam loss timeline for categories of events.

6.2 STS-96/ET-100 -Y Thrust Panel

Figure 12 is a graphic illustration of tabulated foam loss events for the -Y thrust panel on flight STS-96. White lines in the figure enclose vented areas. Figure 13 shows the number of events recorded during each 0.5-sec time interval and the total number of events from T+90 sec. There were 250 total foam loss events recorded. A fifth-order polynomial trend line for the number of events counted per each 0.5 sec indicates a peak value at approximately T+115 sec. The maximum number of events recorded during any 0.5-sec interval was 12. Figure 14 shows the timeline for vented and nonvented foam loss events. Figure 15 illustrates the timeline for accumulated foam loss events in each category. The longitudinal rib section encompasses a majority of the foam loss events. There were no recorded ramp events.

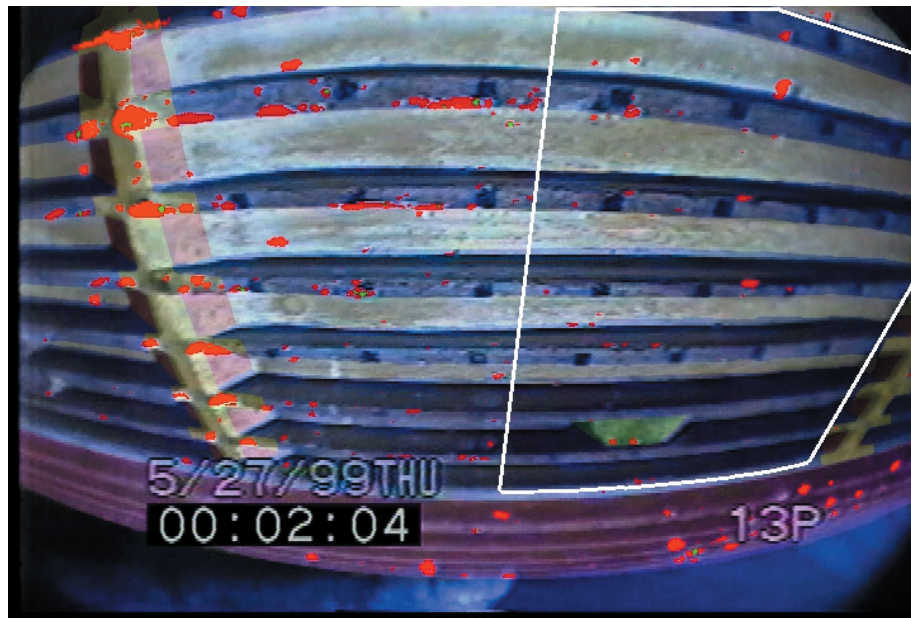


Figure 12. STS-96 -Y thrust panel.

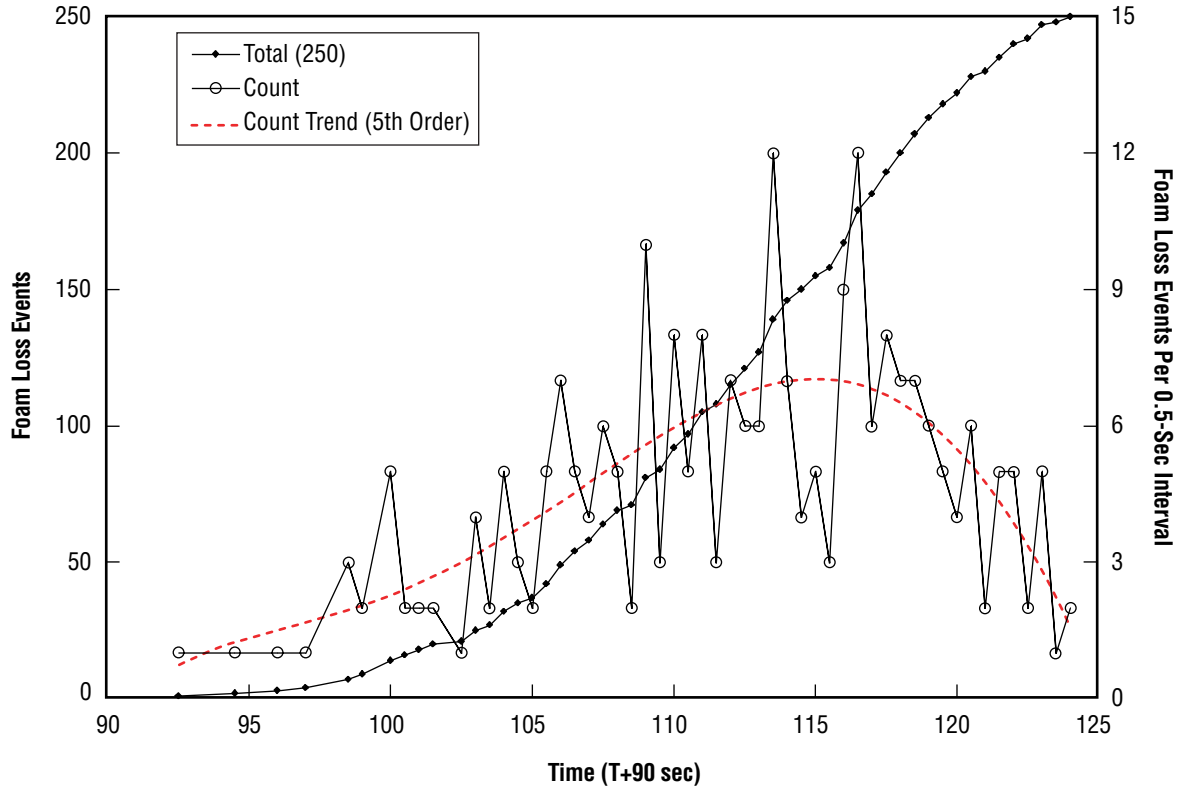


Figure 13. STS-96 -Y thrust panel: Foam loss event timeline.

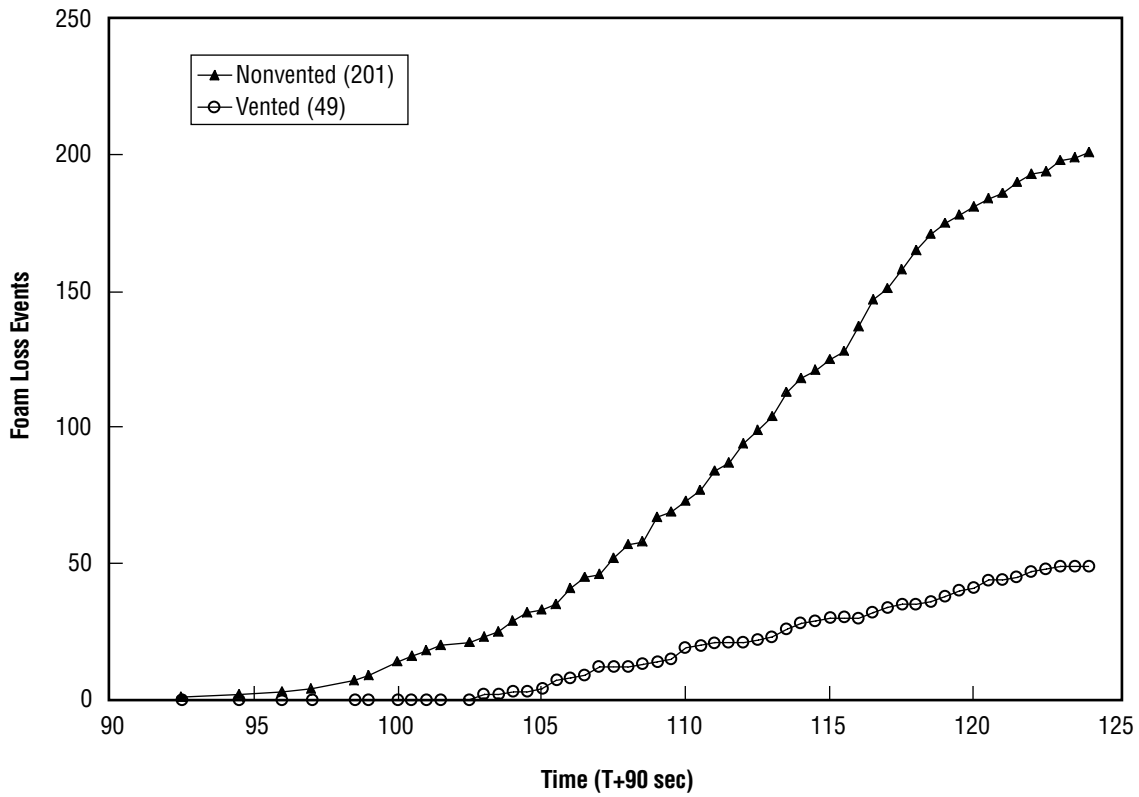


Figure 14. STS-96 -Y thrust panel: Foam loss timeline for vented and nonvented areas.

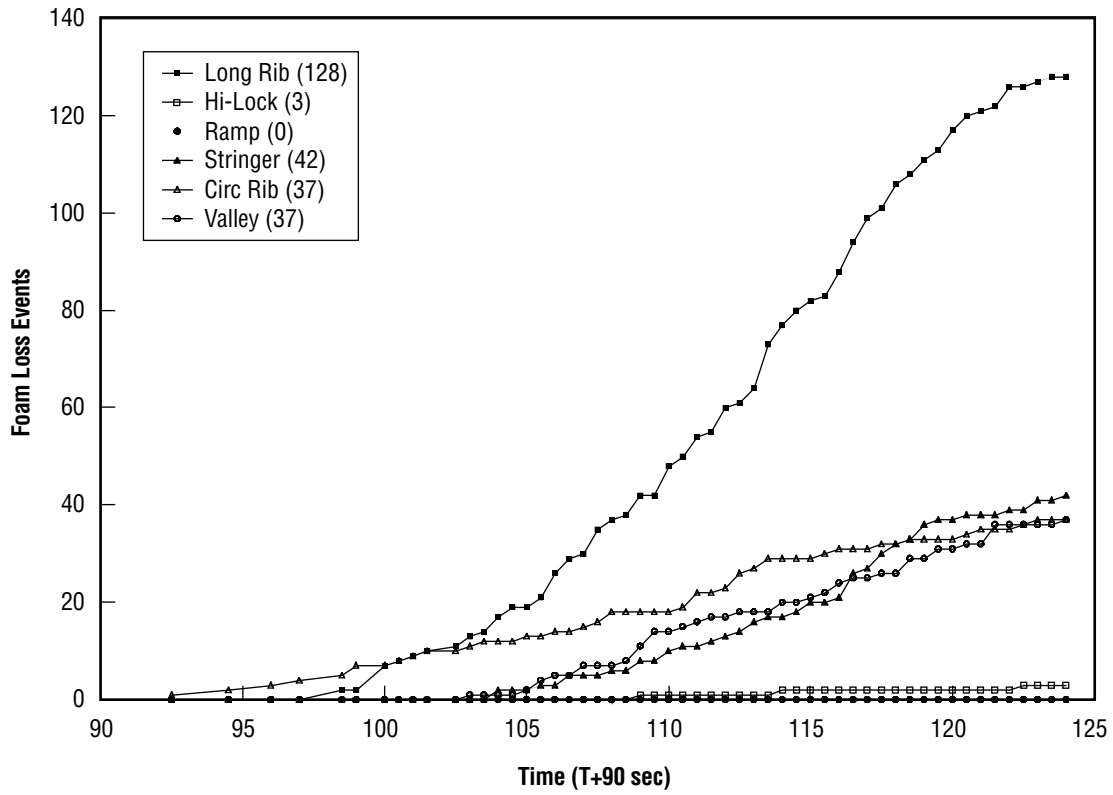


Figure 15. STS-96 -Y thrust panel: Foam loss timeline for categories of events.

6.3 STS-96/ET-100 +Y Thrust Panel

Figure 16 illustrates the tabulated foam loss events on the +Y thrust panel for flight STS-96/ET-100. White lines in the figure enclose vented areas. Figure 17 shows the number of events recorded during each 0.5-sec time interval and the total number of events from T+90 sec. There were 632 total foam loss events recorded. A fifth-order polynomial trend line for the number of events counted per each 0.5 sec indicates a peak value at approximately T+110 sec. The maximum number of events recorded during any 0.5-sec interval was 32. Figure 18 shows the timeline for vented and nonvented foam loss events. Figure 19 illustrates the accumulated foam loss events in each category versus time.

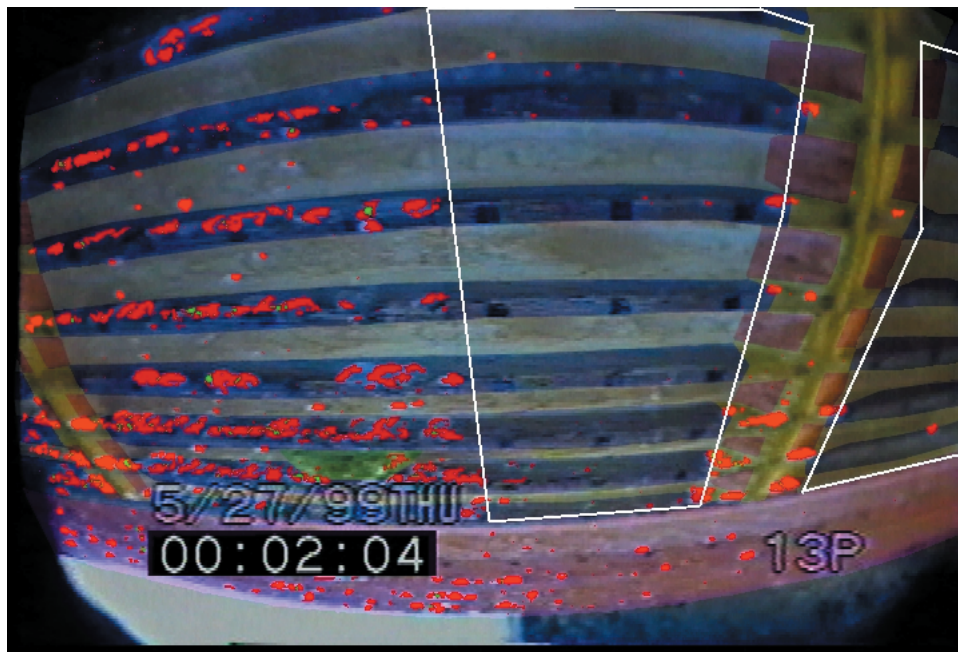


Figure 16. STS-96 +Y thrust panel.

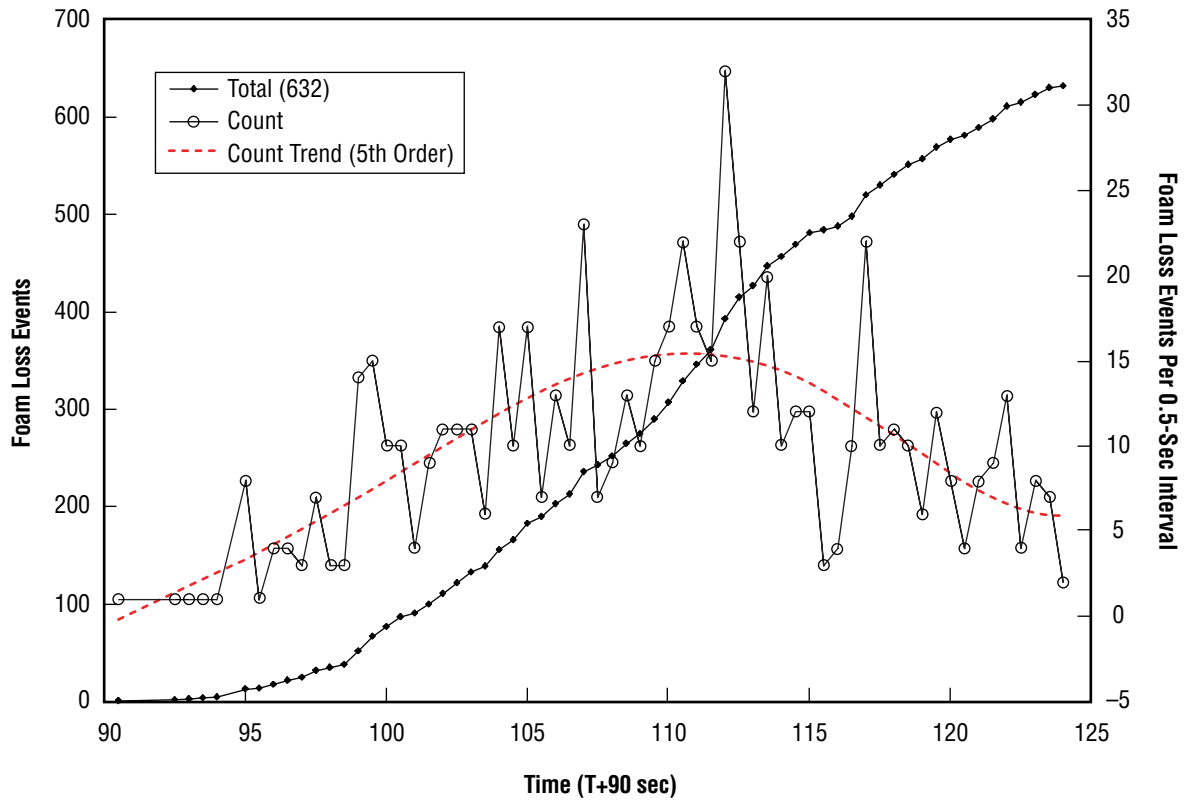


Figure 17. STS-96 +Y thrust panel: Foam loss event timeline.

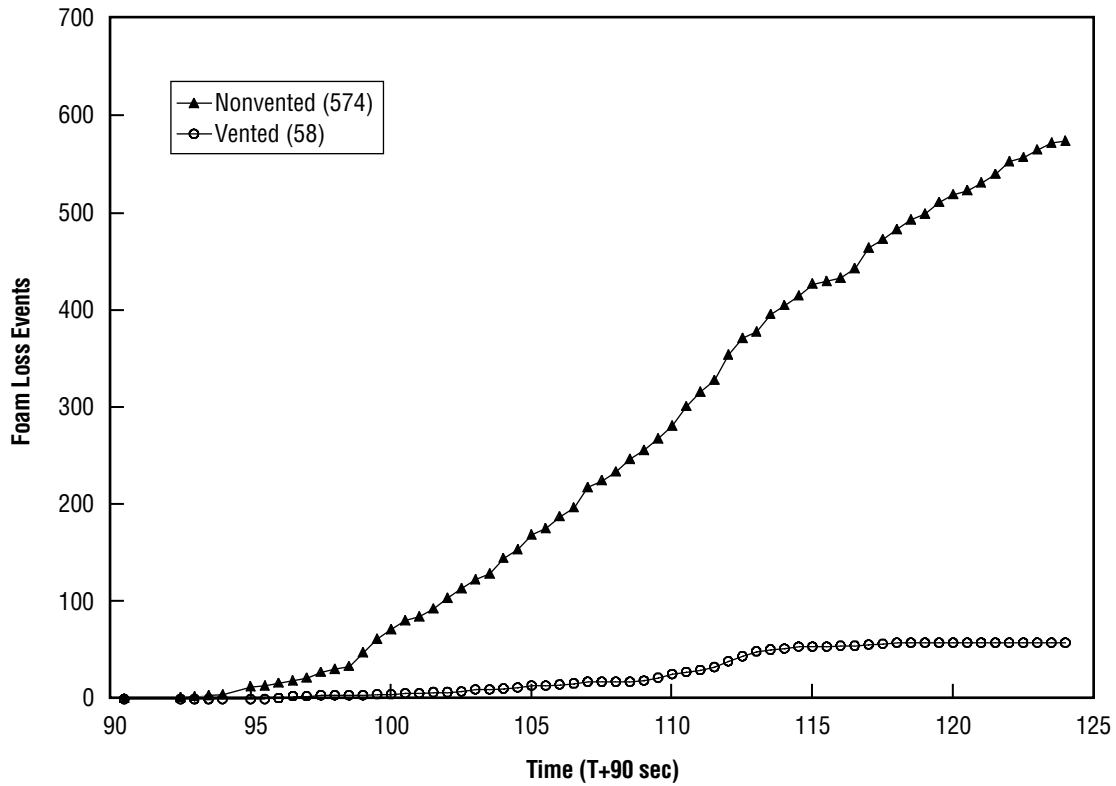


Figure 18. STS-96 +Y thrust panel: Foam loss timeline for vented and nonvented areas.

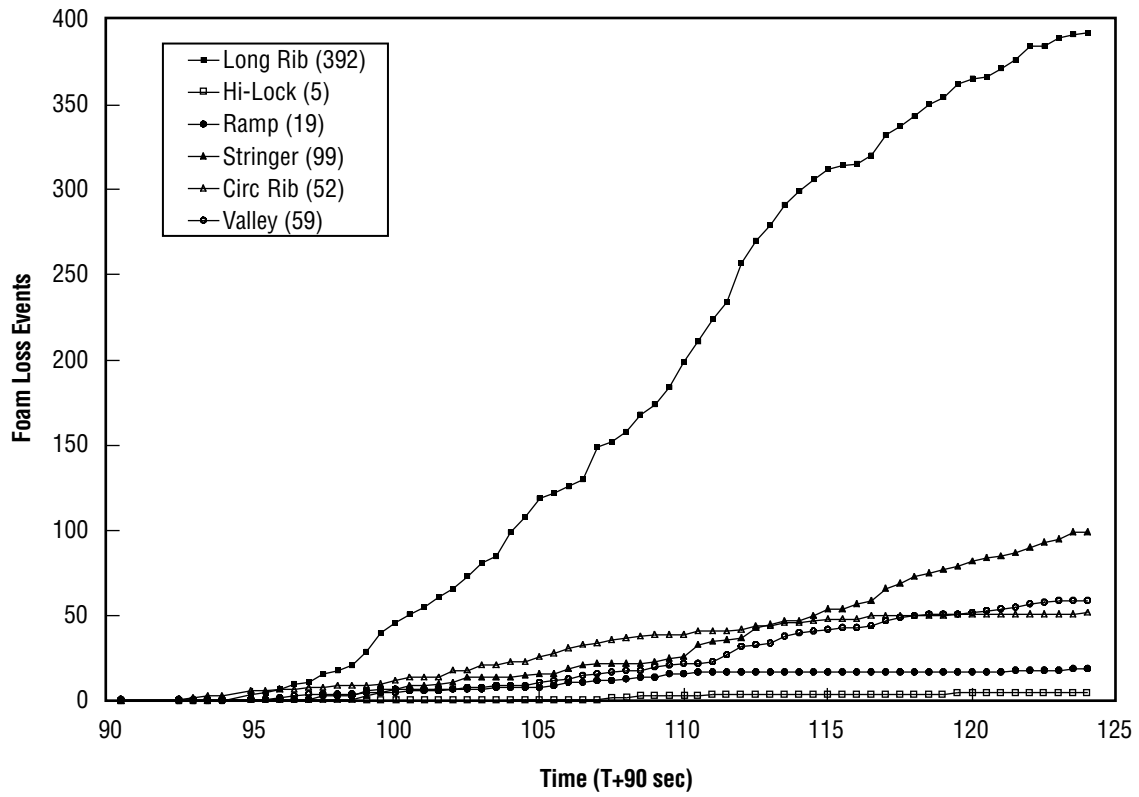


Figure 19. STS-96 +Y thrust panel: Foam loss timeline for categories of events.

6.4 STS-93/ET-99 -Y Thrust Panel

Figure 20 illustrates all tabulated foam loss events on the -Y thrust panel of the ET for flight STS-93/ET-99. White lines in this figure enclose vented areas. There were 144 total foam loss events recorded. The number of events recorded during each 0.5-sec time interval and the total number of events from T+90 sec are shown in figure 21. Using a third-order polynomial approximation to trend the count data, the count trend line in this figure indicates a probable maximum of activity at about T+113 sec. The maximum number of recorded events during any 0.5-sec interval was eight. Figure 22 compares vented and nonvented areas. Figure 23 illustrates the accumulated foam loss events in each category versus time. The longitudinal rib section encompasses a majority of the foam loss events.

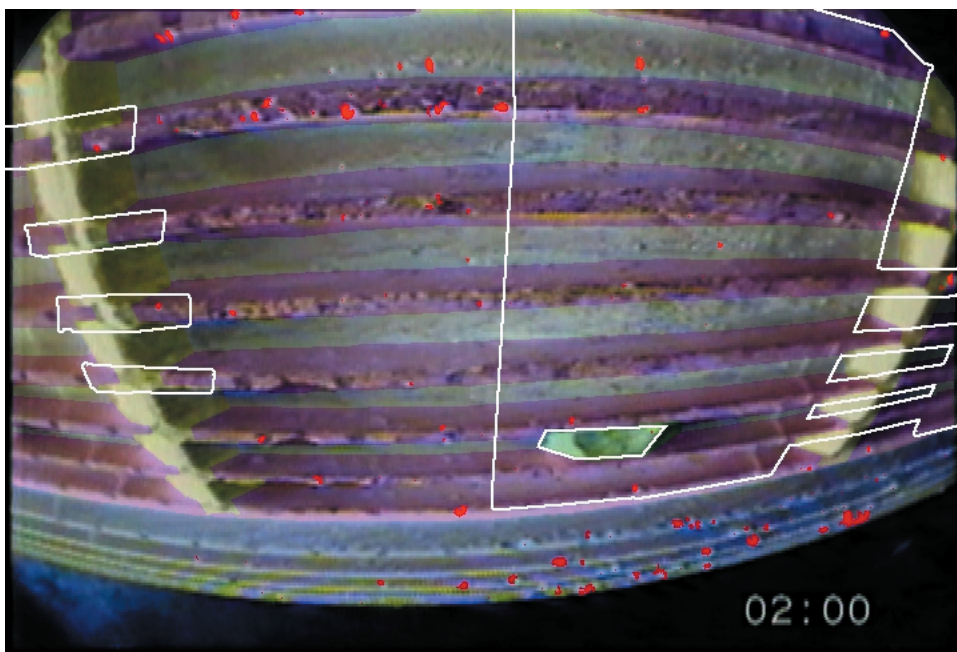


Figure 20. STS-93 -Y thrust panel.

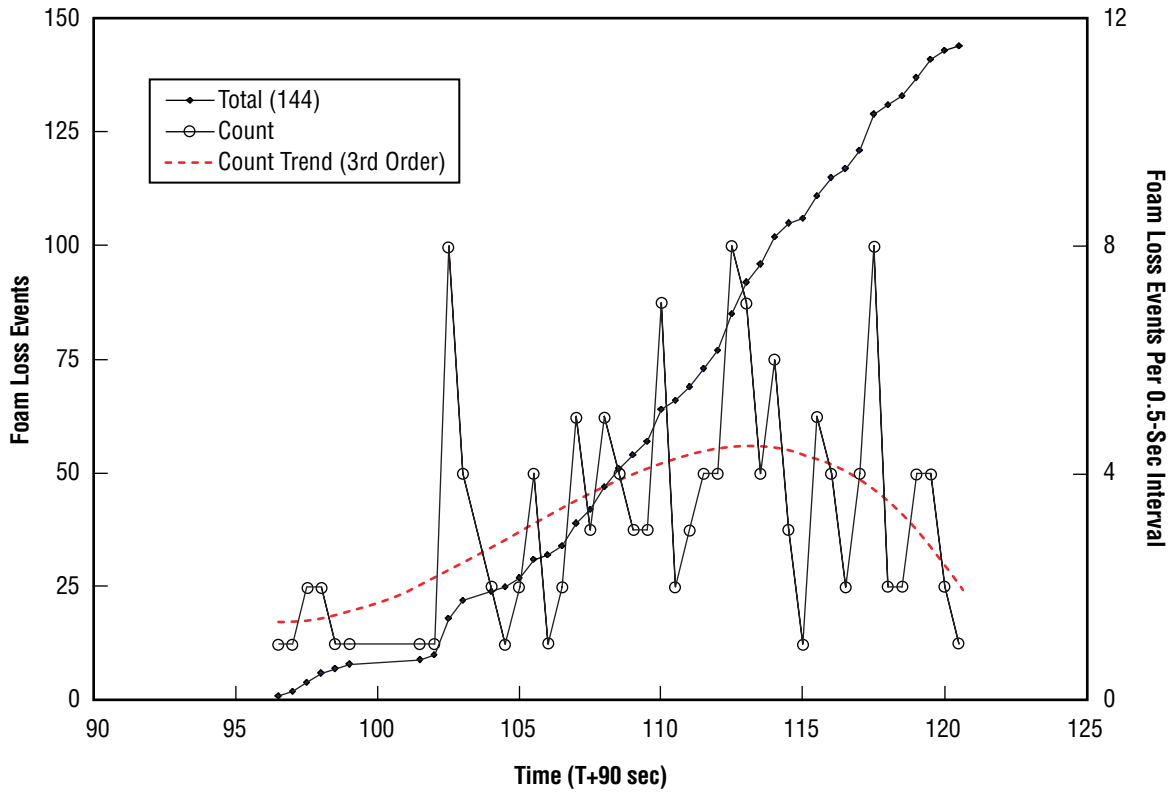


Figure 21. STS-93 -Y thrust panel: Foam loss event timeline.

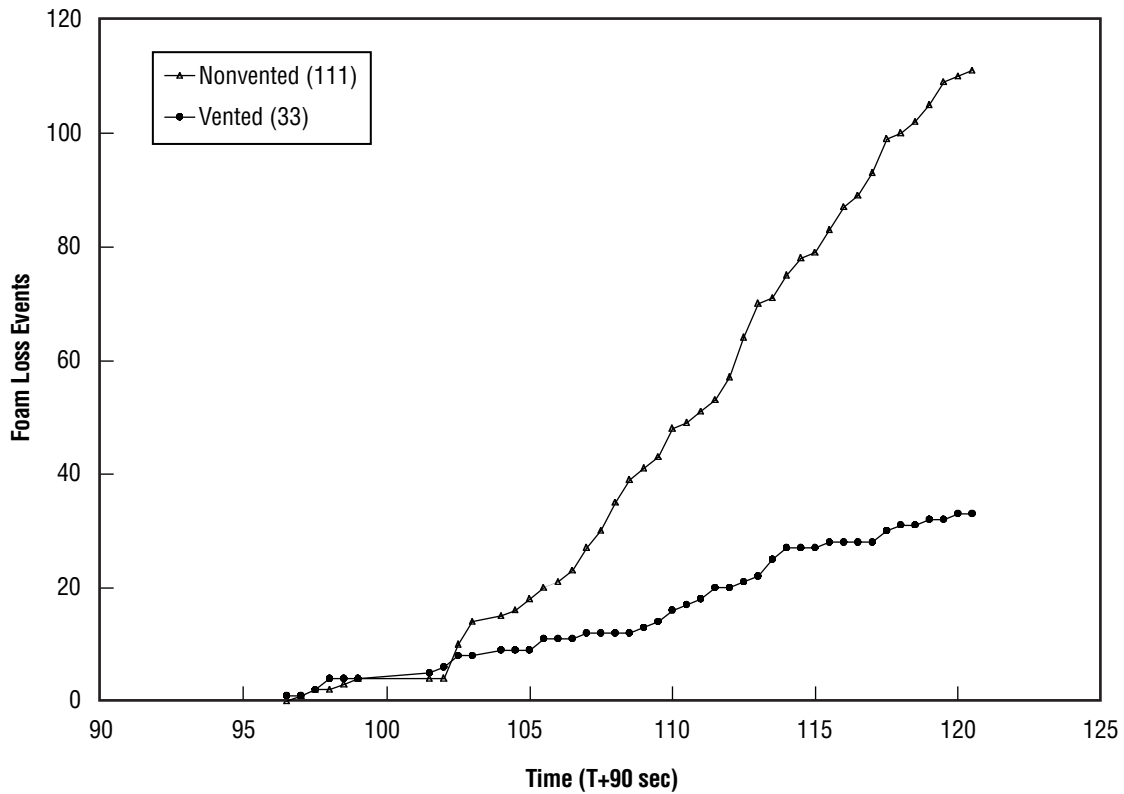


Figure 22. STS-93 -Y thrust panel: Foam loss timeline for vented and nonvented areas.

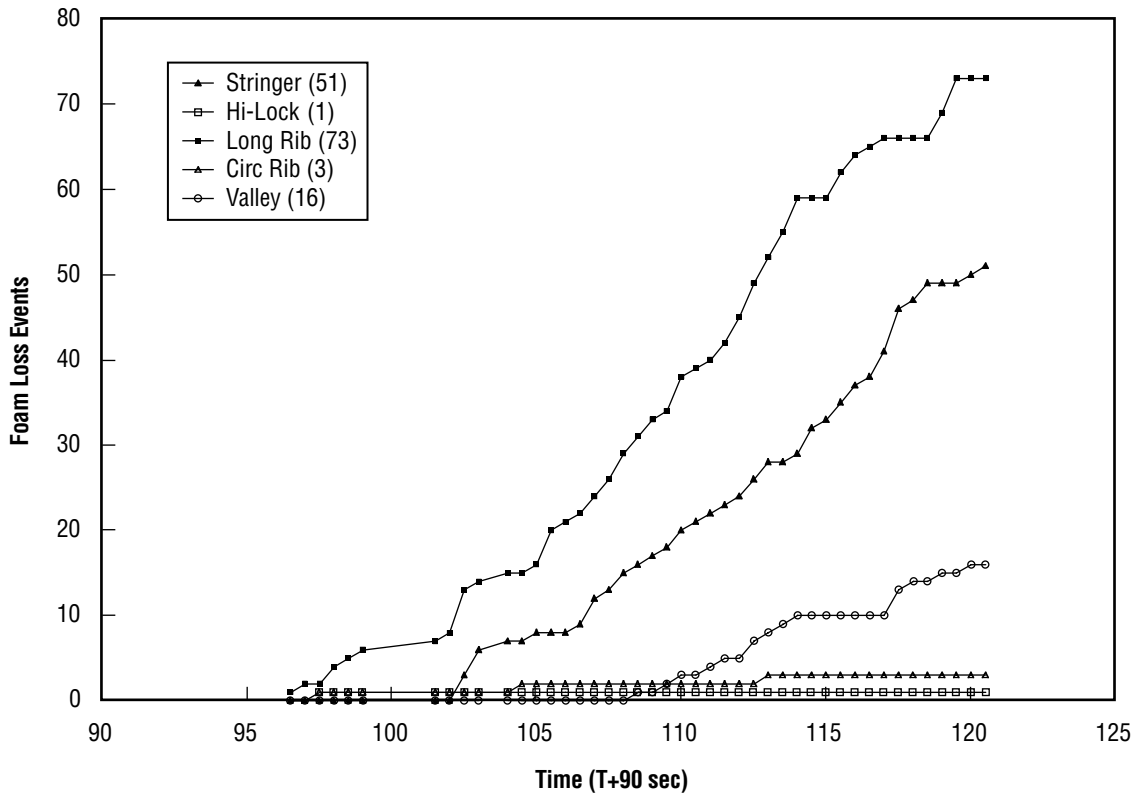


Figure 23. STS-93 -Y thrust panel: Foam loss timeline for categories of events.

6.5 STS-93/ET-99 +Y Thrust Panel

Figure 24 illustrates all tabulated foam loss events on the +Y thrust panel of the ET for flight STS-93/ET-99. White lines in the figure enclose vented areas. There were 119 total foam loss events recorded. The number of events recorded during each 0.5-sec time interval and the total number of events from T+90 sec are shown in figure 25. Using a fifth-order polynomial approximation to trend the count data, the maximum foam loss activity appears to peak near T+110 sec and then revive near T+120 sec. The maximum number of events recorded during any 0.5-sec time interval was 11. Figure 26 compares vented and nonvented areas. Figure 27 illustrates the timeline for accumulated foam loss in each category.

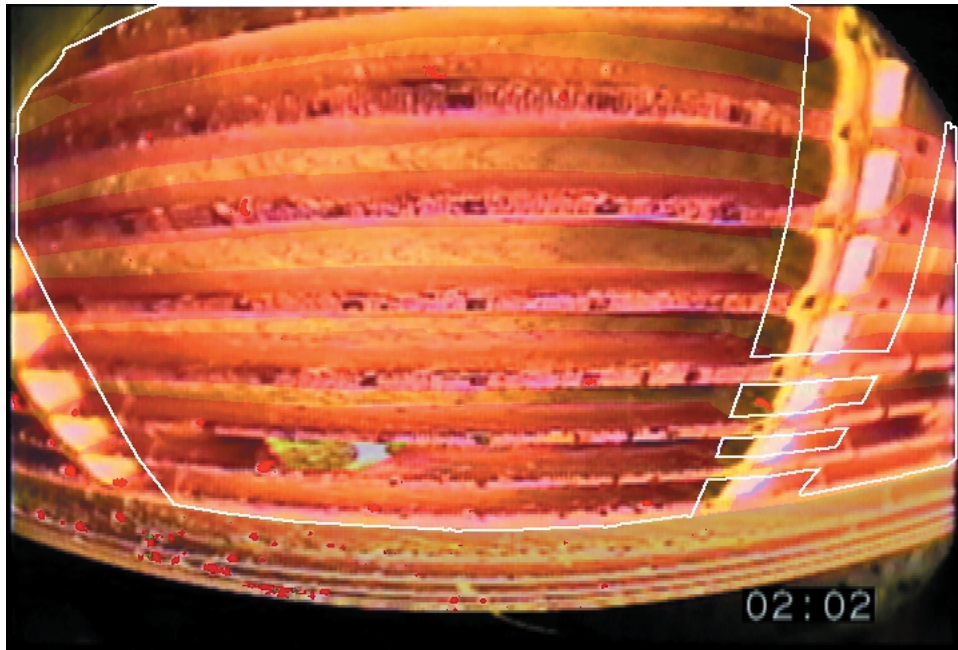


Figure 24. STS-93 +Y thrust panel.

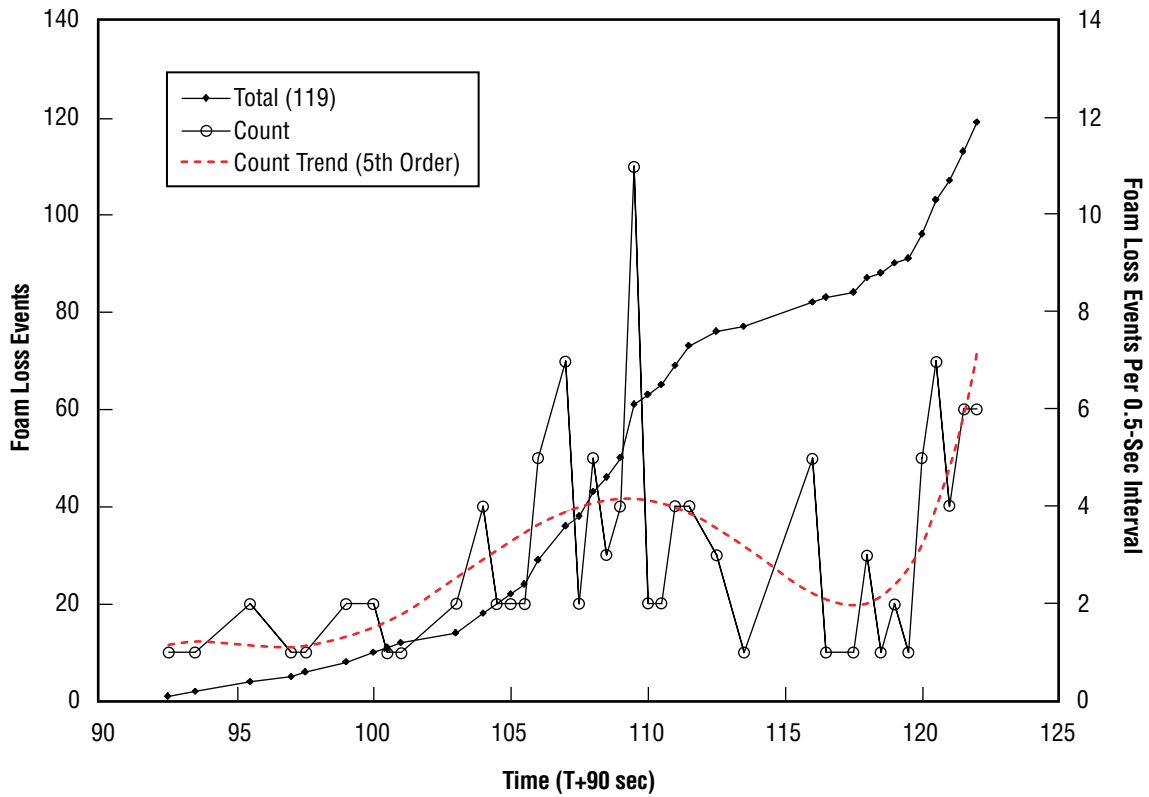


Figure 25. STS-93 +Y thrust panel: Foam loss event timeline.

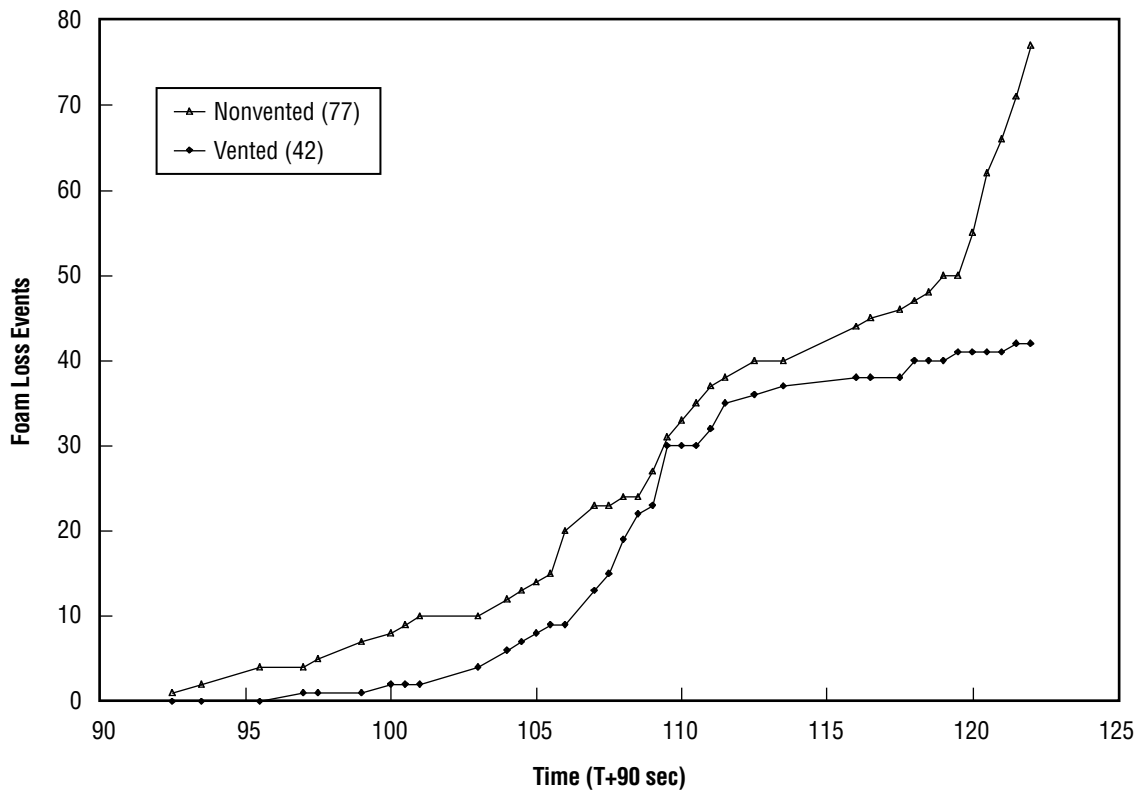


Figure 26. STS-93 +Y thrust panel: Foam loss timeline for vented and nonvented areas.

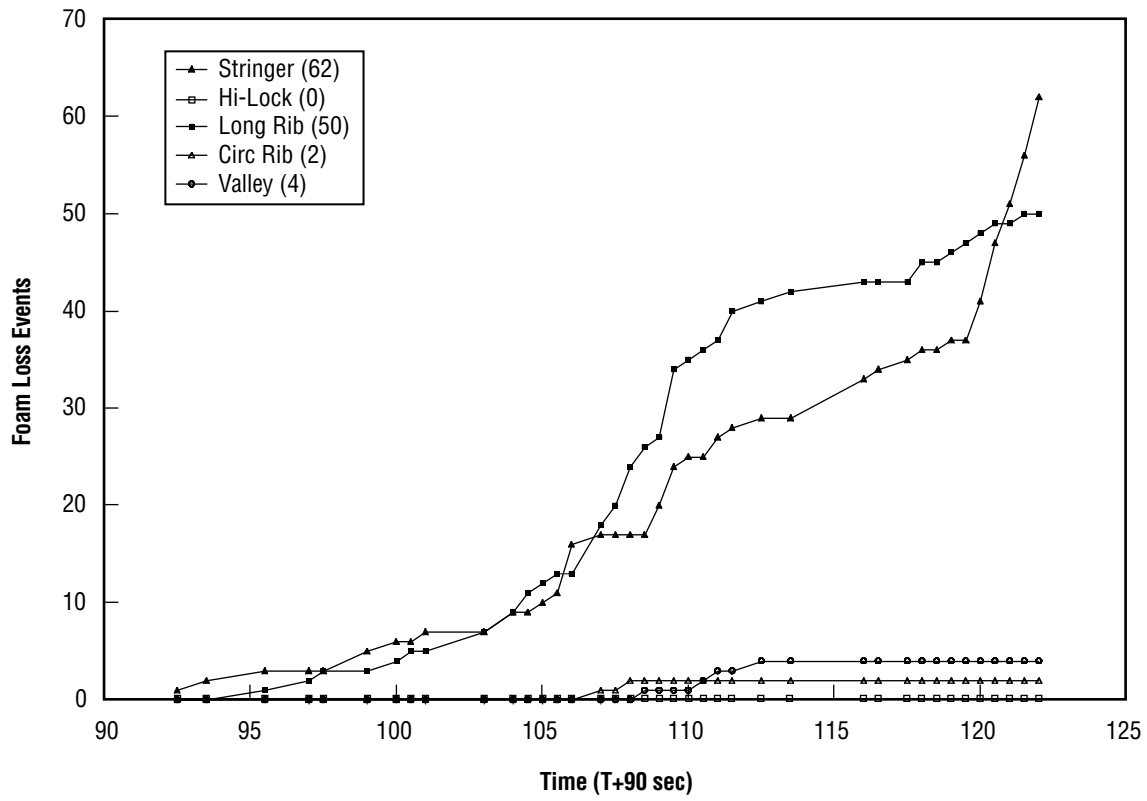


Figure 27. STS-93 +Y thrust panel: Foam loss timeline for categories of events.

6.6 STS-103 -Y Thrust Panel

Figure 28 illustrates all tabulated foam loss events on the -Y thrust panel of the ET for flight STS-103. White lines in the figure enclose vented areas. There were 39 total foam loss events recorded. The number of events recorded during each 0.5-sec time interval and the total number of events from approximately T+90 sec are shown in figure 29. Using a fourth-order polynomial approximation to trend the count data, the maximum foam loss activity appears to peak just after T+110 sec. The maximum number of events recorded during any 0.5-sec time interval was four. Figure 30 compares vented and nonvented areas. Figure 31 illustrates the timeline for accumulated foam loss in each category.

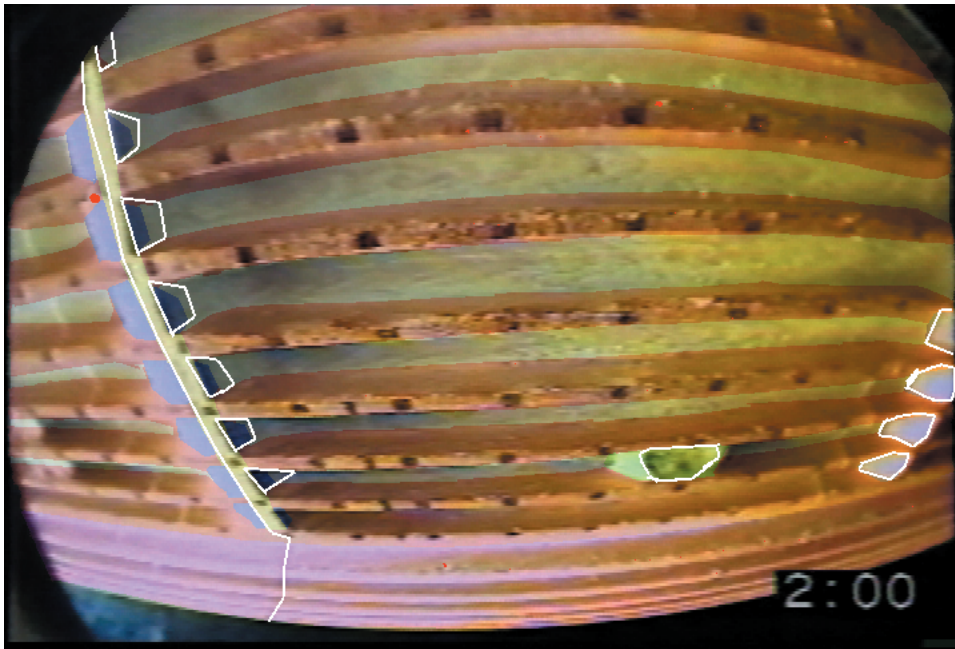


Figure 28. STS-103 -Y thrust panel.

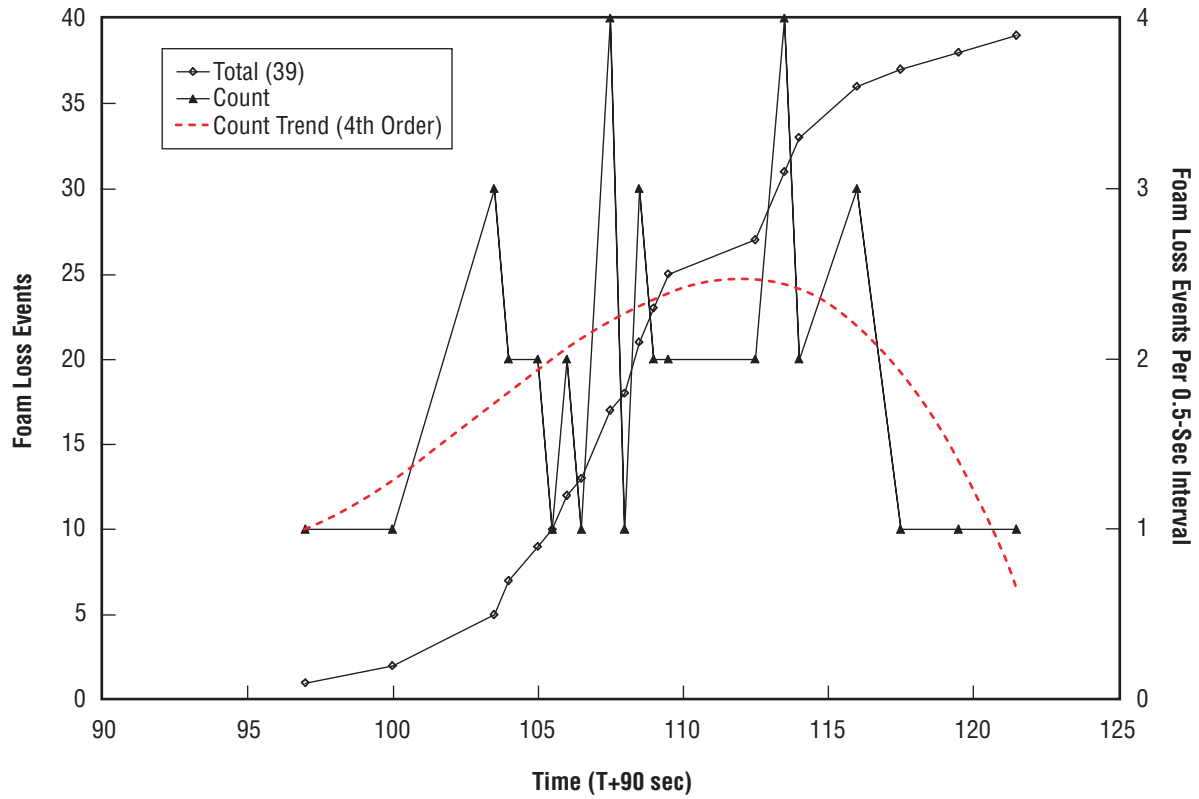


Figure 29. STS-103 -Y thrust panel: Foam loss event timeline.

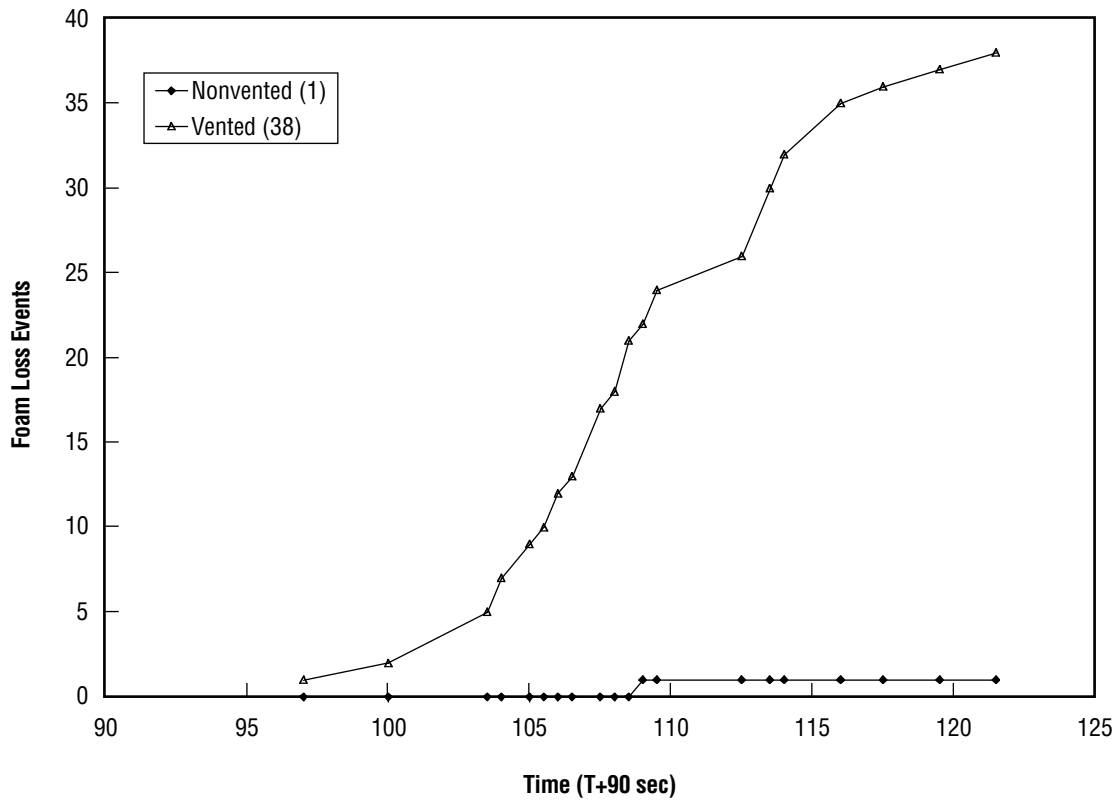


Figure 30. STS-103 -Y thrust panel: Foam loss timeline for vented and nonvented areas.

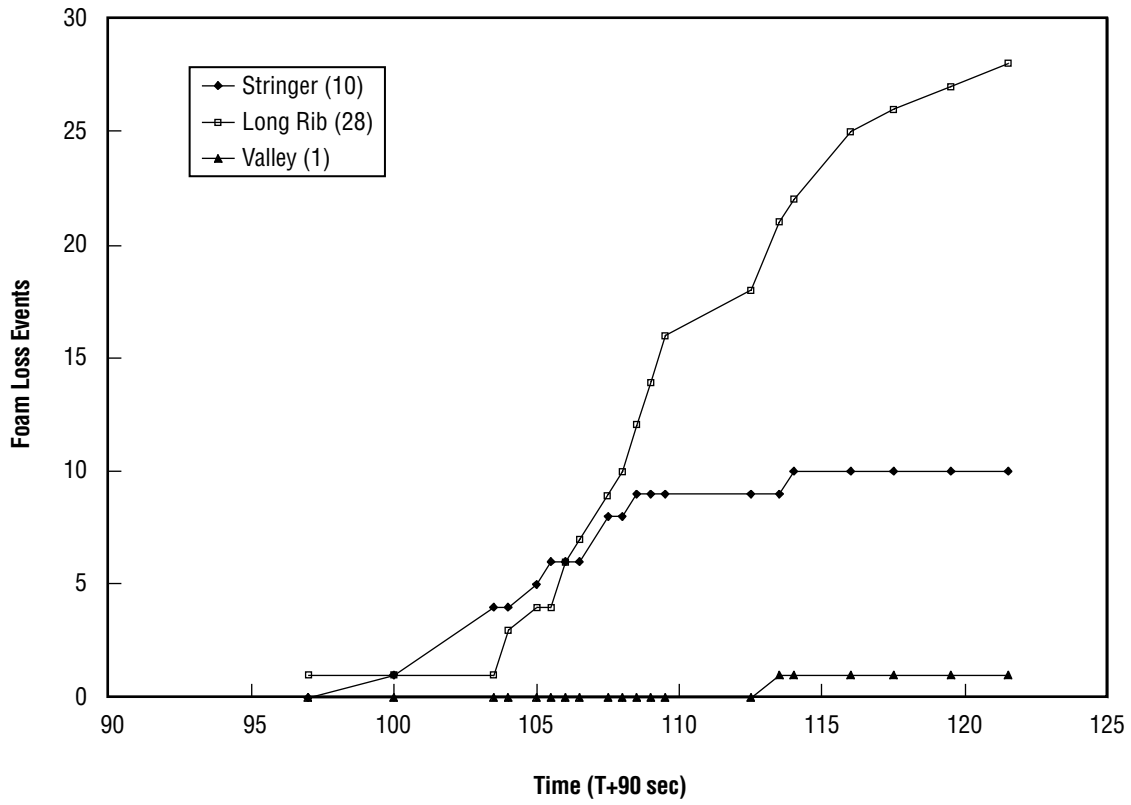


Figure 31. STS-103 -Y thrust panel: Foam loss timeline for categories of events.

6.7 STS-103 +Y Thrust Panel

Figure 32 illustrates all tabulated foam loss events on the +Y thrust panel of the ET for flight STS-103. White lines in the figure enclose vented areas. There were 63 total foam loss events recorded. The number of events recorded during each 0.5-sec time interval and the total number of events from approximately T+90 sec are shown in figure 33. Using a fifth-order polynomial approximation to trend the count data, the maximum foam loss activity appears to peak before T+110 sec. The maximum number of events recorded during any 0.5-sec time interval was six. Figure 34 compares vented and non-vented areas. Figure 35 illustrates the timeline for accumulated foam loss in each category.

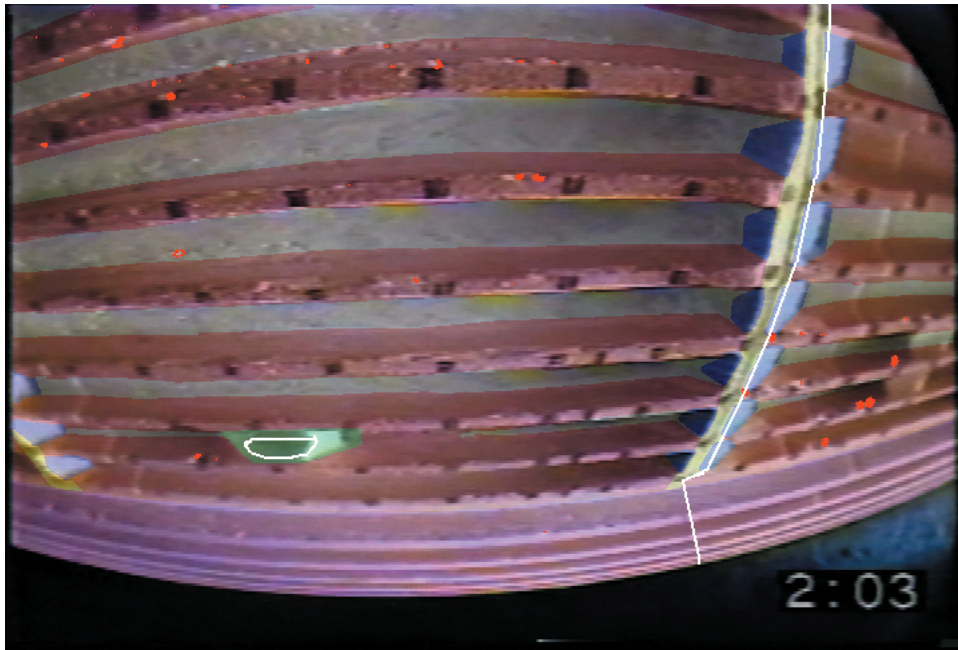


Figure 32. STS-103 +Y thrust panel.

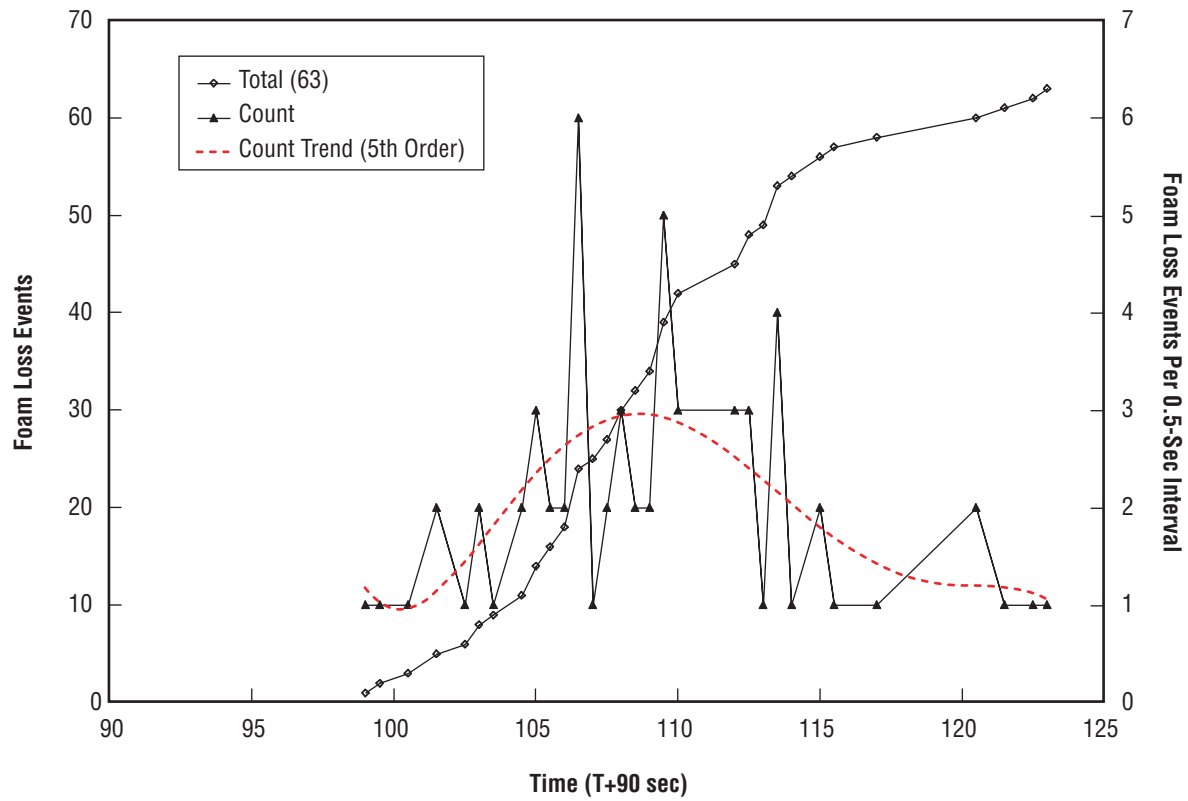


Figure 33. STS-103 +Y thrust panel: Foam loss event timeline.

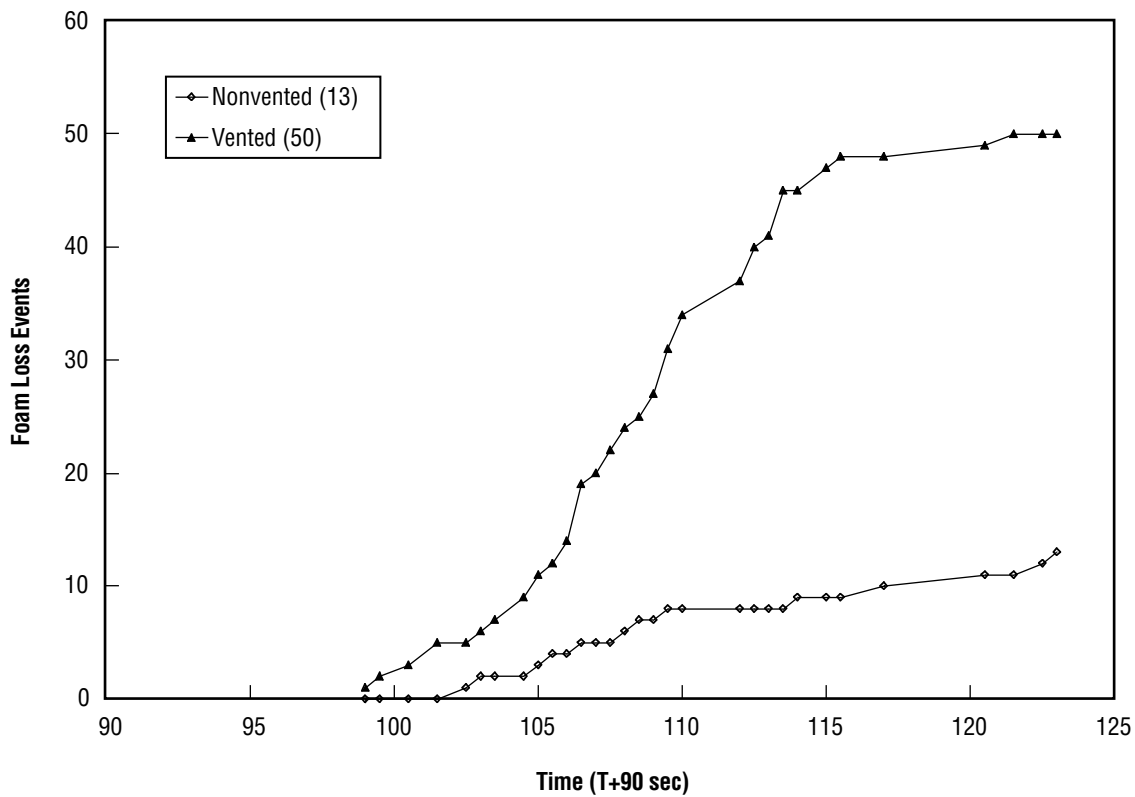


Figure 34. STS-103 +Y thrust panel: Foam loss timeline for vented and nonvented areas.

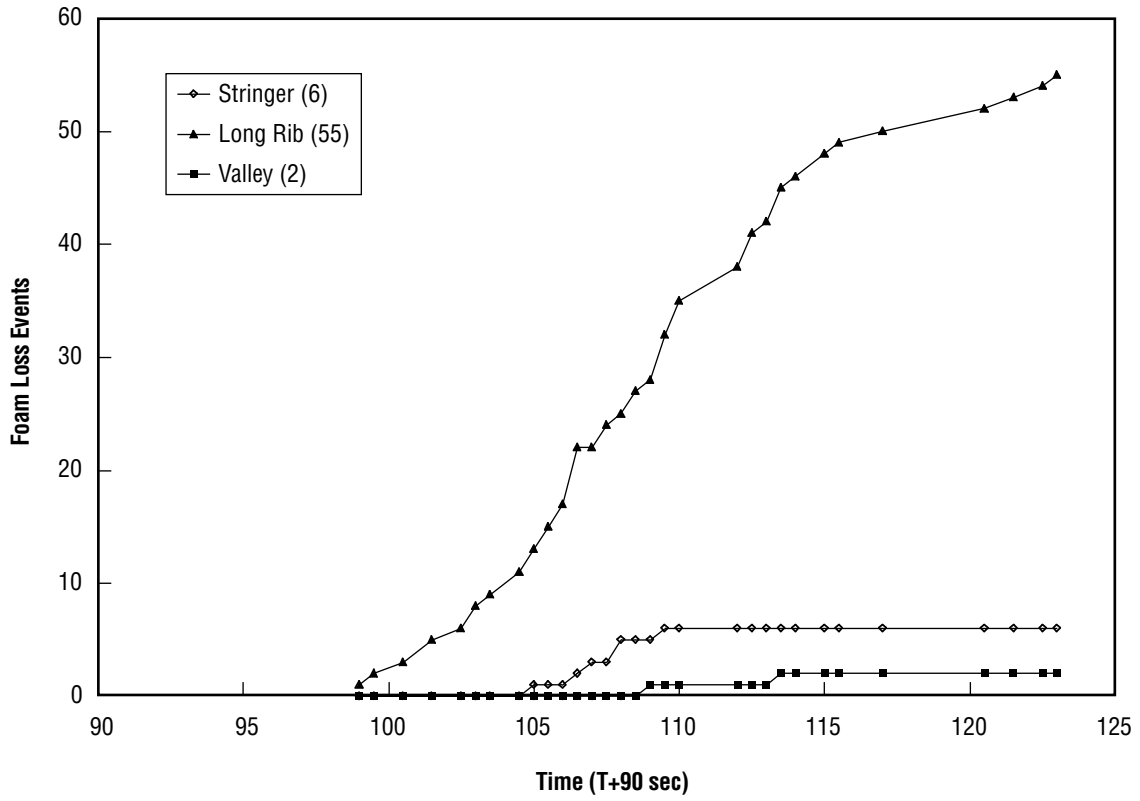


Figure 35. STS-103 +Y thrust panel: Foam loss timeline for categories of events.

6.8 STS-101 -Y Thrust Panel

Figure 36 illustrates all tabulated foam loss events on the -Y thrust panel of the ET for flight STS-101. White lines in the figure enclose vented areas. There were 100 total foam loss events recorded. The number of events recorded during each 0.5-sec time interval and the total number of events from approximately T+90 sec are shown in figure 37. Using a fourth-order polynomial approximation to trend the count data, the maximum foam loss activity appears to peak just after T+110 sec. The maximum number of events recorded during any 0.5-sec time interval was seven. Figure 38 compares vented and nonvented areas. Figure 39 illustrates the timeline for accumulated foam loss in each category.

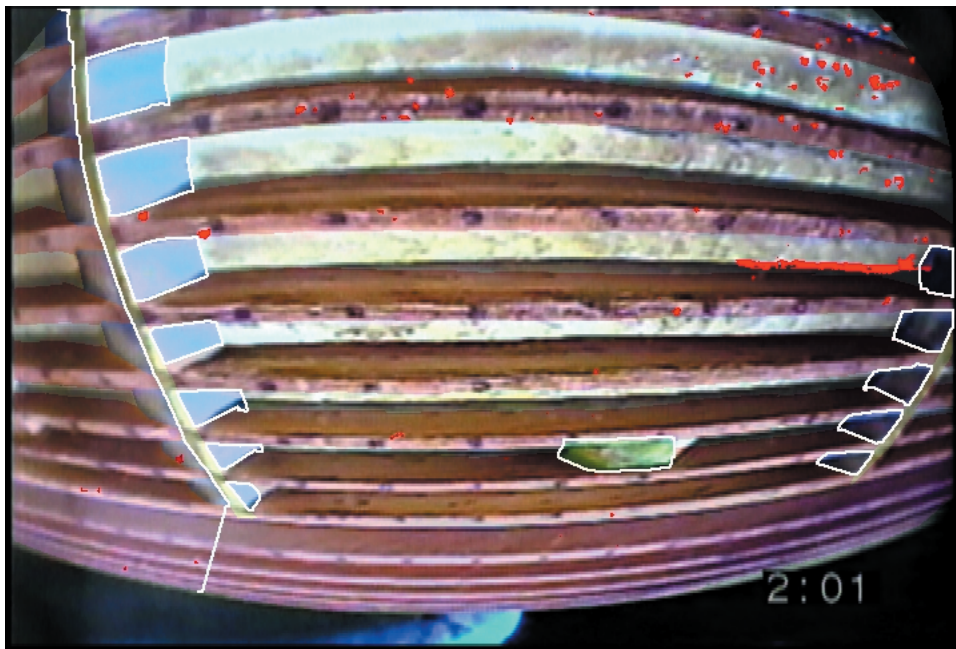


Figure 36. STS-101 -Y thrust panel.

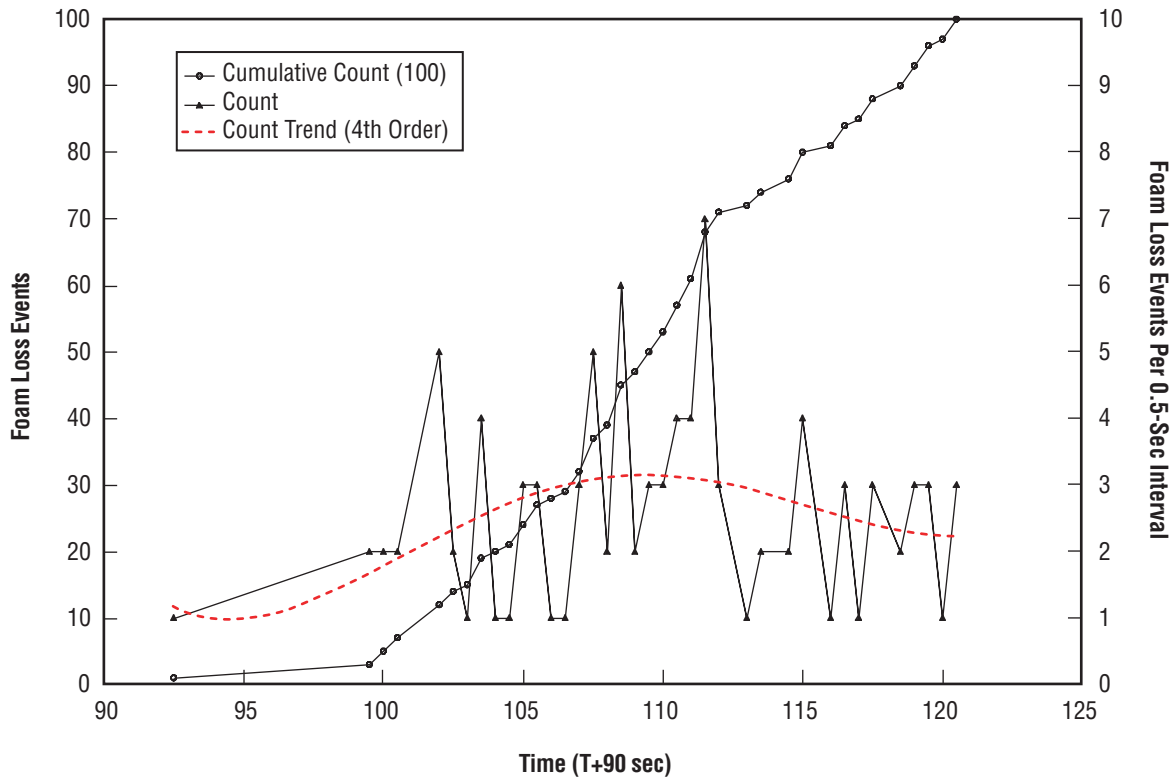


Figure 37. STS-101 -Y thrust panel: Foam loss event timeline.

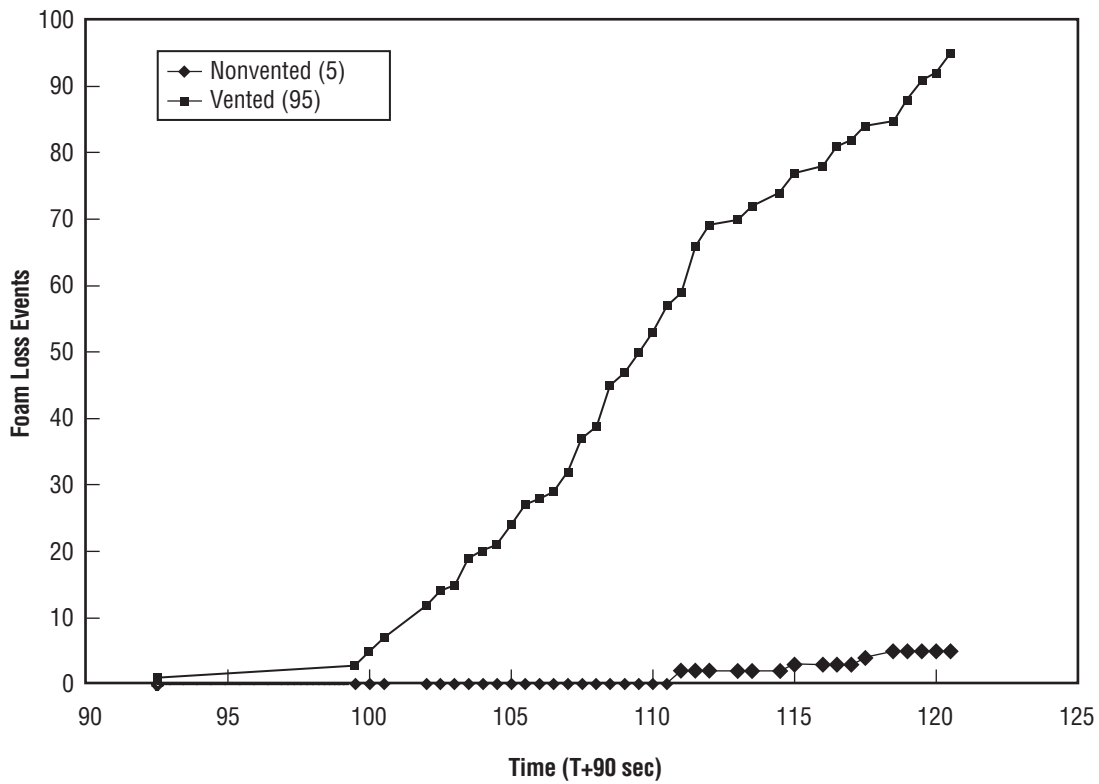


Figure 38. STS-101 -Y thrust panel: Foam loss timeline for vented and nonvented areas.

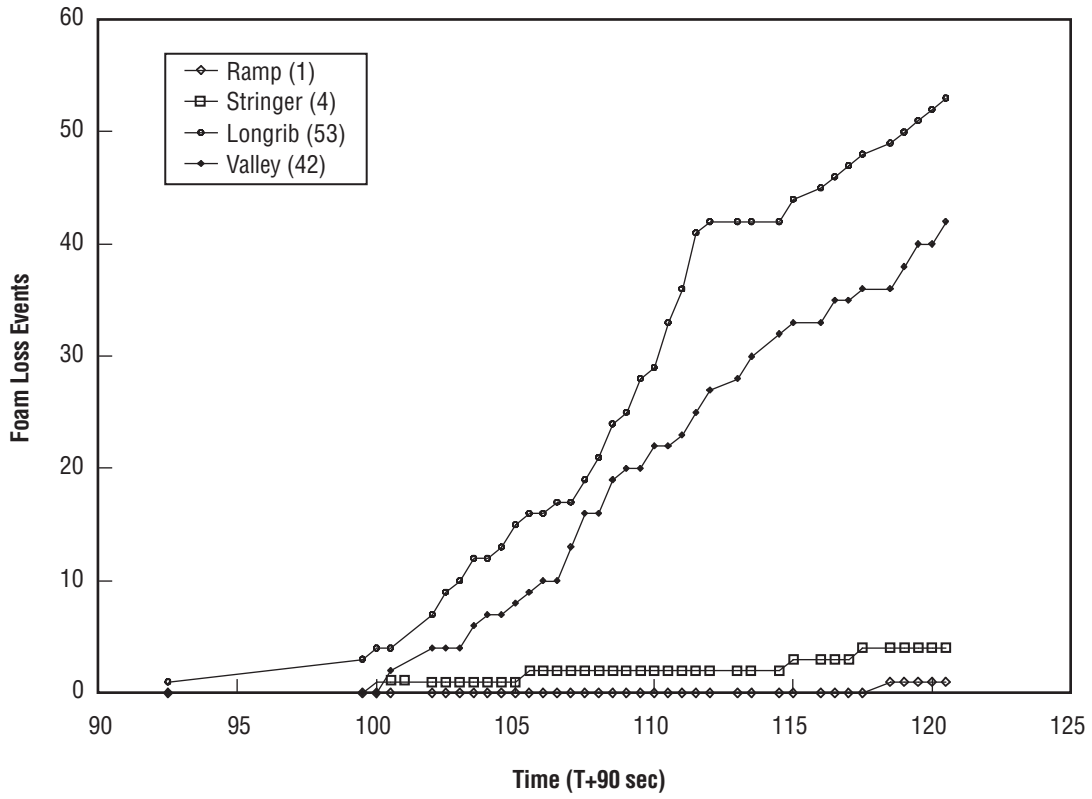


Figure 39. STS-101 -Y thrust panel: Foam loss timeline for categories of events.

6.9 STS-101 +Y Thrust Panel

Figure 40 illustrates all tabulated foam loss events on the +Y thrust panel of the ET for flight STS-101. White lines in the figure enclose vented areas. There were 258 total foam loss events recorded. The number of events recorded during each 0.5-sec time interval and the total number of events from approximately T+90 sec is shown in figure 41. Using a third-order polynomial approximation to trend the count data, the maximum foam loss activity appears to peak at approximately T+110 sec. The maximum number of events recorded during any 0.5-sec time interval was 23. Figure 42 compares vented and nonvented areas. Figure 43 illustrates the timeline for accumulated foam loss in each category.

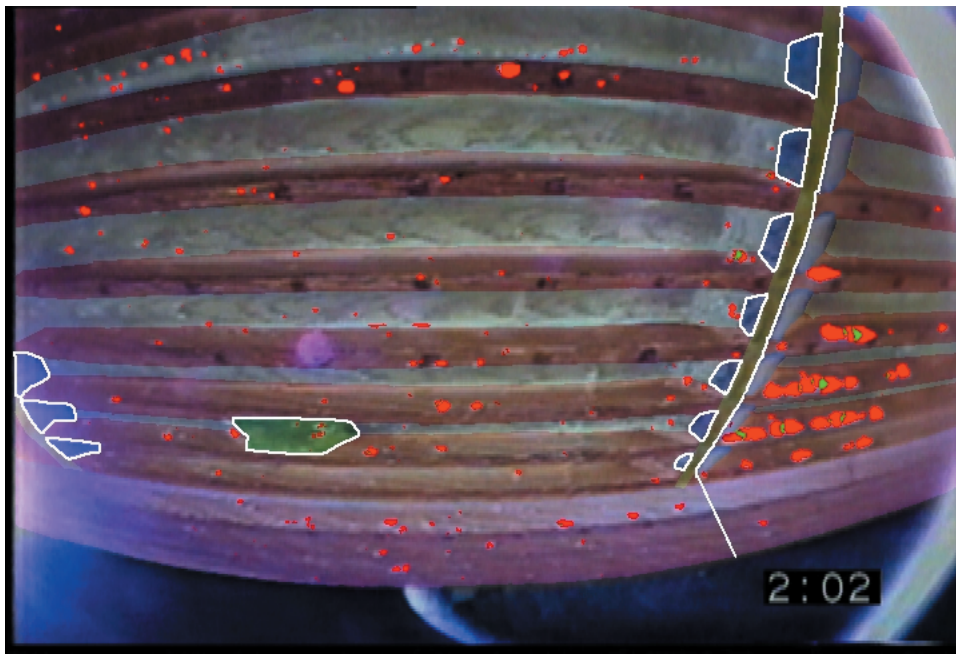


Figure 40. STS-101 +Y thrust panel.

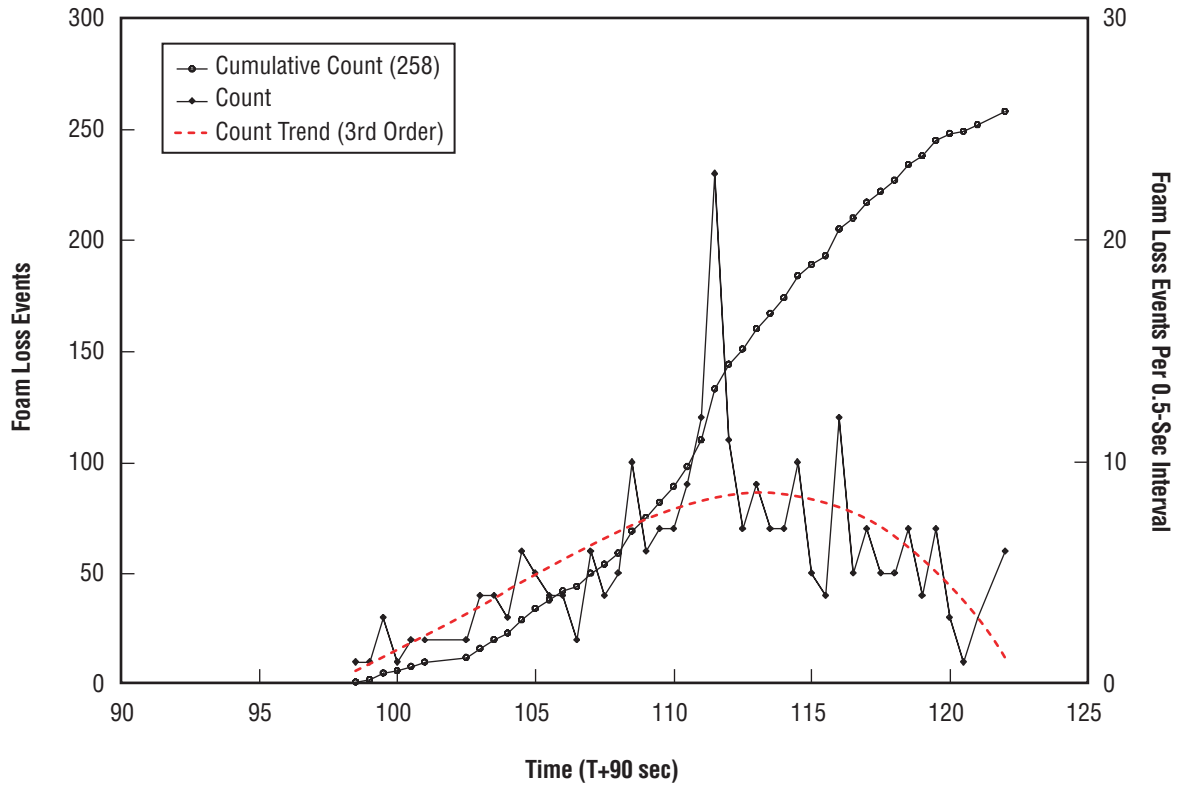


Figure 41. STS-101 +Y thrust panel: Foam loss event timeline.

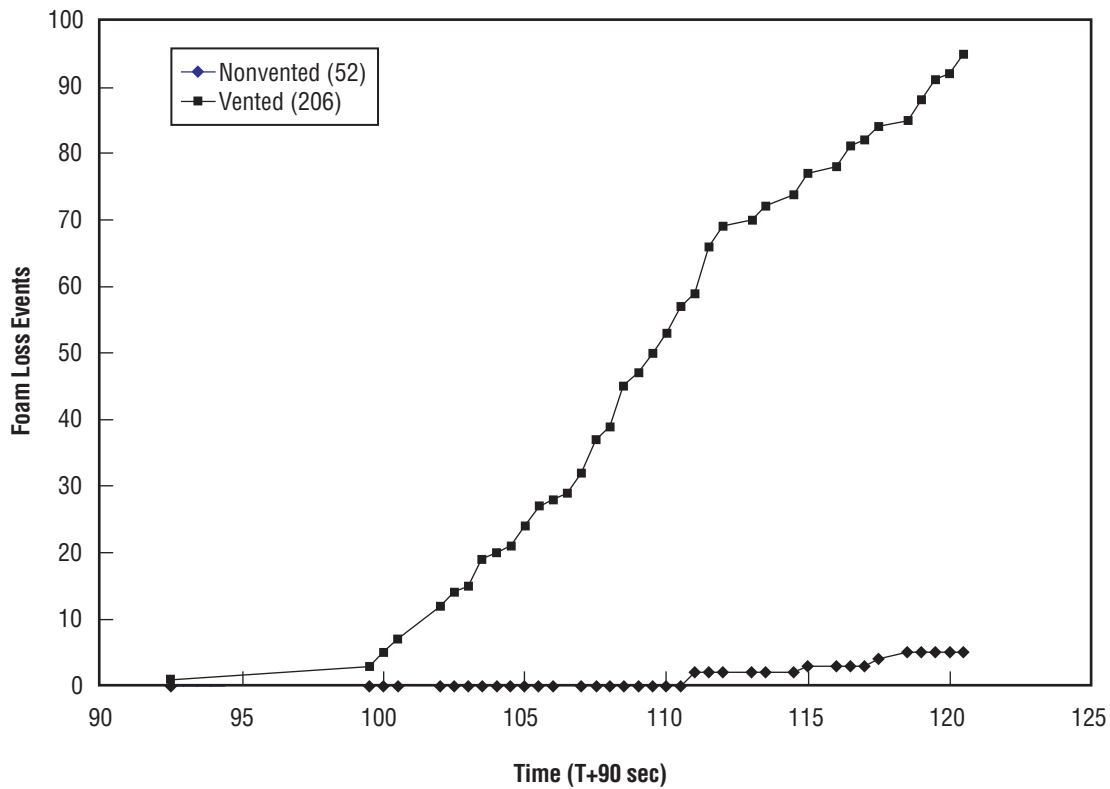


Figure 42. STS-101 +Y thrust panel: Foam loss timeline for vented and nonvented areas.

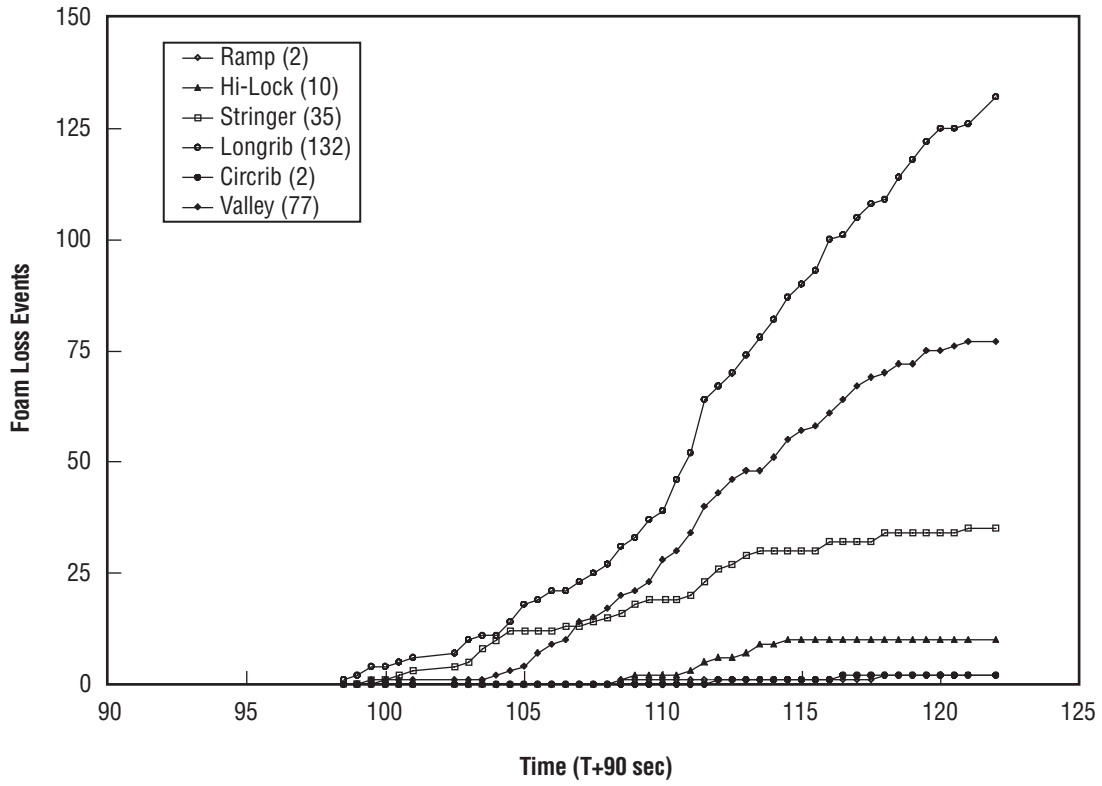


Figure 43. STS-101 +Y thrust panel: Foam loss timeline for categories of events.

7. DISCUSSION

The method described in this Technical Memorandum for revealing permanent changes in the ET surface may be used in any sequence of digitized images as an aid in establishing the time and location of events that leave an observable permanent change. This method is easily applied, yielding a sequence of images in which only permanent change occurs in the sequence of original images. This method is an excellent aid in evaluation of permanent changes occurring in a video sequence as it allows the analyst to focus on removal of nonrelated events rather than detection of events. This method is far superior to directly observing video images and noting changes, especially in situations where a large number of events are occurring.

One comparison of the present difference file counting method with the previous simple method, counting foam loss events directly from videotape images, is illustrated in table 1. The data are from the STS-96 -Y thrust panel. In each time period, the number of events counted is equal to or greater in the difference file counting method. This was the case in nearly all SRB videos reviewed.

Table 1. Counting methods differences.

Time Period	Simple Counting Method			Difference File Counting Method		
	Vented	Unvented	Total	Vented	Unvented	Total
90-94.5	0	2	2	0	2	2
95-104.5	0	16	16	3	30	33
105-114.5	20	27	47	26	89	115
115-125	5	30	35	20	80	100
Total	25	75	100	49	201	250

Due to inherent video noise and the need for engineering judgment to determine the level of surface change that signifies a foam loss event, the absolute numbers of foam loss events counted varies with the group making the count. Under these conditions, general trends in the data become more important. Inspection of the data in table 1 indicates that the general trend of the count between these two sources is essentially the same.

One goal of camera coverage of foam loss events was to help determine the effectiveness of methods of foam preparation. The technique of foam venting as a method of decreasing foam loss events is increasingly applied over four flights, as illustrated in figures 44 and 45. Later flights showed decreases in foam loss events in both +Y and -Y thrust panels.

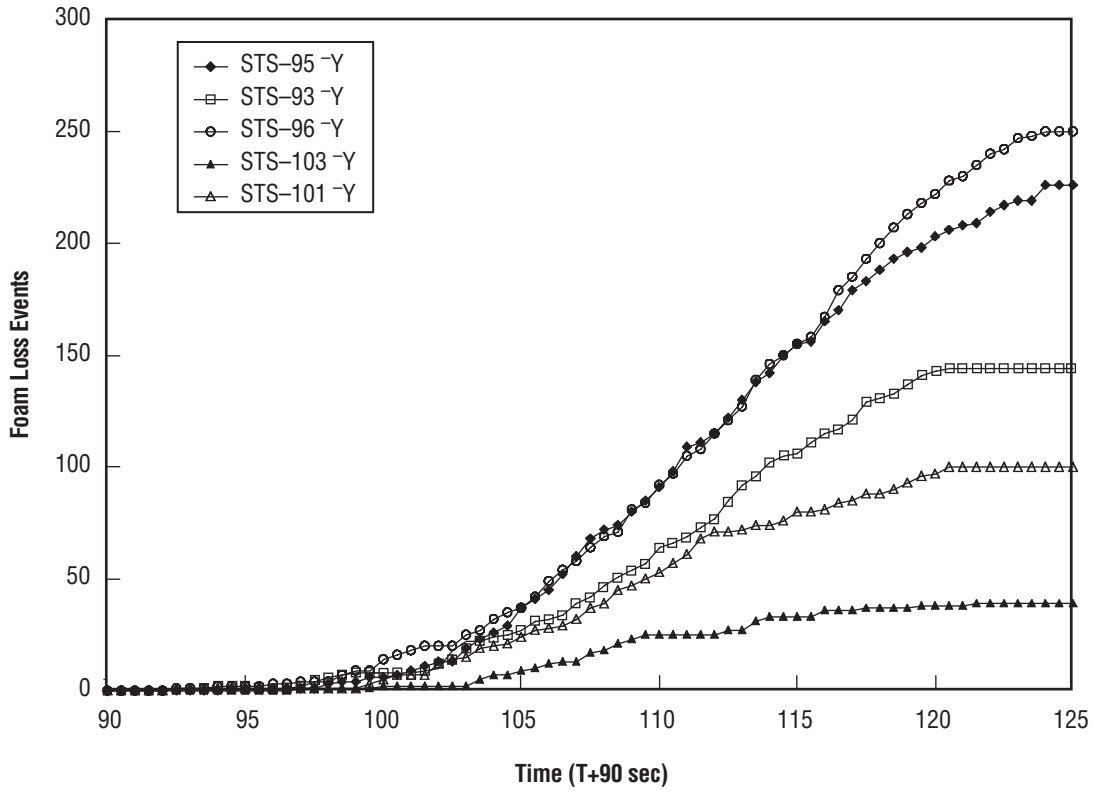


Figure 44. Foam loss comparison for -Y thrust panels.

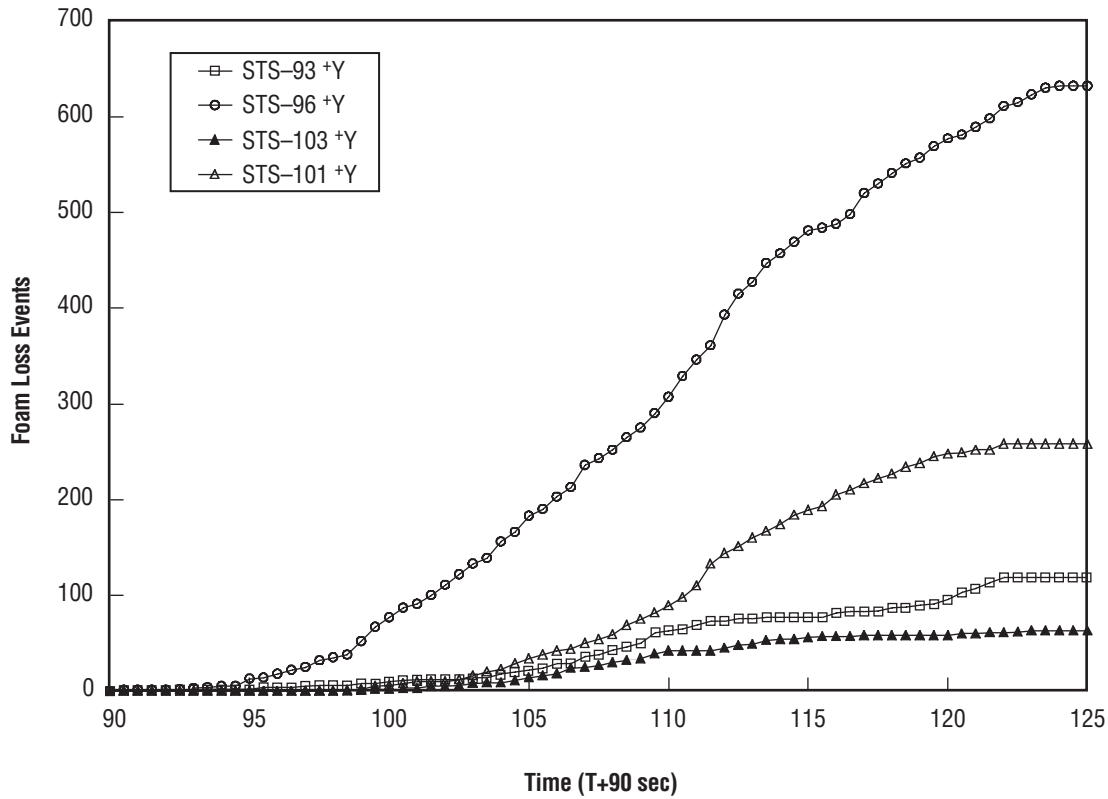


Figure 45. Foam loss comparison for +Y thrust panels.

There are several areas for improvement of the event detection method. It was observed that a number of foam loss events occurred which were not revealed by this process. The difference level between successive frames for these particular events was low; i.e., below a gray-scale level of 20. While most of these events were insignificant, several events were of considerable size. An improved method might use a local threshold as opposed to a global threshold. Related to this problem was the fluctuation of the global intensity level. This phenomena caused a majority of the pixels of a frame to be included into the difference image and made automated discovery of foam loss events unfeasible. To compensate for this problem, an offset from the local mean intensity level in one frame to the local mean intensity level in the succeeding frame could be calculated and used to weigh the local changes from these means against each other.

Also, camera motion could be periodic and of a different frequency than the frequency obtained from the time interval between selected frames, yielding consistent areas of change in difference frames. A method of eliminating such changes should be included in automating the process. This problem is related to the noticeable image creep that occurred over the processed sequence of images. To eliminate this problem, each divot had to be evaluated and followed to ensure that it was not relabeled as growth of a previous foam loss event and mistakenly counted again.

Video dropouts and horizontal bars of varying color yield areas where no information can be gained from the image and induce a large change area in differencing with the succeeding image. It was found that using an adjoining image or duplication of the last image without these imperfections was helpful to avoid these spurious inclusions into the difference image.

BIBLIOGRAPHY

1. Gonzalez, R.C.; and Wintz P.: *Digital Image Processing*, 2nd ed., Addison-Wesley Publishing Company, Reading, MA, pp. 5–6, 1987.
2. Holst, G.C.: *CCD Arrays, Cameras, and Displays*, 2nd ed., JCD Publishing, Winter Park, FL, and SPIE Optical Engineering Press, Bellingham, WA, pp. 15, 149, 1998.
3. Pratt, W.K.: *Digital Image Processing*, 2nd ed., John Wiley & Sons, New York, NY, p. 63, 1991.
4. Williams, C.: *Root Cause of ET Intertank Foam Loss*, Lockheed Martin Internal White Paper, 1999.

REPORT DOCUMENTATION PAGEForm Approved
OMB No. 0704-0188

Public reporting burden for this collection of information is estimated to average 1 hour per response, including the time for reviewing instructions, searching existing data sources, gathering and maintaining the data needed, and completing and reviewing the collection of information. Send comments regarding this burden estimate or any other aspect of this collection of information, including suggestions for reducing this burden, to Washington Headquarters Services, Directorate for Information Operation and Reports, 1215 Jefferson Davis Highway, Suite 1204, Arlington, VA 22202-4302, and to the Office of Management and Budget, Paperwork Reduction Project (0704-0188), Washington, DC 20503

1. AGENCY USE ONLY (Leave Blank)		2. REPORT DATE June 2001	3. REPORT TYPE AND DATES COVERED Technical Memorandum	
4. TITLE AND SUBTITLE Photographic Analysis Technique for Assessing External Tank Foam Loss Events			5. FUNDING NUMBERS	
6. AUTHORS T.J. Rieckhoff, M. Covan,* and J.M. O'Farrell*				
7. PERFORMING ORGANIZATION NAMES(S) AND ADDRESS(ES) George C. Marshall Space Flight Center Marshall Space Flight Center, AL 35812			8. PERFORMING ORGANIZATION REPORT NUMBER M-1006	
9. SPONSORING/MONITORING AGENCY NAME(S) AND ADDRESS(ES) National Aeronautics and Space Administration Washington, DC 20546-0001			10. SPONSORING/MONITORING AGENCY REPORT NUMBER NASA/TM-2001-210880	
11. SUPPLEMENTARY NOTES Prepared for Vehicle and Systems Development Department, Space Transportation Directorate *United Space Alliance, Huntsville, AL				
12a. DISTRIBUTION/AVAILABILITY STATEMENT Unclassified-Unlimited Subject Category 35 Nonstandard Distribution			12b. DISTRIBUTION CODE	
13. ABSTRACT (Maximum 200 words) A video camera and recorder were placed inside the solid rocket booster forward skirt in order to view foam loss events over an area on the external tank (ET) intertank surface. In this Technical Memorandum, a method of processing video images to allow rapid detection of permanent changes indicative of foam loss events on the ET surface was defined and applied to accurately count, categorize, and locate such events.				
14. SUBJECT TERMS photographic analysis, image processing, solid rocket booster, thermal protection system (TPS), divots, feature recognition			15. NUMBER OF PAGES 52	
			16. PRICE CODE	
17. SECURITY CLASSIFICATION OF REPORT Unclassified	18. SECURITY CLASSIFICATION OF THIS PAGE Unclassified	19. SECURITY CLASSIFICATION OF ABSTRACT Unclassified	20. LIMITATION OF ABSTRACT Unlimited	